Available on line at www.rac.es/racsam
Applied Mathematics

REVISTA DE LA REAL ACADEMIA DE CIENCIAS
EXACTAS, FISICAS Y NATURALES.
SERIE A: MATEMATICAS
Madrid (España / Spain)

RACSAM **104** (1), 2010, 153–196. DOI:10.5052/RACSAM.2010.13

Qualitative properties and approximation of solutions of Bingham flows: on the stabilization for large time and the geometry of the support

J. I. Díaz, R. Glowinski, G. Guidoboni and T. Kim

Abstract We study the transient flow of an isothermal and incompressible Bingham fluid. Similar models arise in completely different contexts as, for instance, in material science, image processing and differential geometry. For the two-dimensional flow in a bounded domain we show the extinction in a finite time even under suitable nonzero external forces. We also consider the special case of a three-dimensional domain given as an infinitely long cylinder of bounded cross section. We give sufficient conditions leading to a scalar formulation on the cross section. We prove the stabilization of solutions, when t goes to infinity, to the solution u_∞ of the associated stationary problem, once we assume a suitable convergence on the right hand forcing term. We give some sufficient conditions for the extinction in a finite time of solutions of the scalar problem. We show that, at least under radially symmetric conditions, when the stationary state is not trivial, $u_\infty \neq 0$, there are cases in which the stabilization to the stationary solution needs an infinite time to take place. We end the paper with some numerical experiences on the scalar formulation. In particular, some of those experiences exhibit an instantaneous change of topology of the support of the solution: when the support of the initial datum is formed by two disjoint balls, but closed enough, then, instantaneously, for any $t > 0$, the support of the solution $u(\,\cdot\,, t)$ becomes a connected set. Some other numerical experiences are devoted to the study of the "profile" of the solution and its extinction time.

Propiedades cualitativas y aproximación de las soluciones de problemas de fluidos de Bingham: sobre la estabilización para tiempos grandes y la geometría del soporte de las soluciones

Resumen. Consideramos el flujo transitorio de un fluido de Bingham isotérmico e incompresible. Modelos similares se plantean en contextos completamente diferentes como, por ejemplo, en ciencias de los materiales, tratamiento de imágenes y geometría diferencial. Para el flujo en un dominio bidimensional mostramos la extinción en tiempo finito, incluso bajo adecuadas fuerzas externas no nulas. Consideramos tambien el caso especial del dominio tridimensional dado por un cilindro infinitamente largo de

Submitted by Amable Liñán.
Received: December 13, 2009. *Accepted*: January 13, 2010
Keywords: Bingham flows, propagation of the support, stabilzation, finite extinction time, numerical experiences
Mathematics Subject Classifications: 35K55, 35R35, 35K85, 35B30, 35B35, 65N30, 68U20, 76A05

sección transversal acotada. Damos condiciones suficientes que conducen a una formulación escalar sobre el dominio transversal. Probamos la estabilización de las soluciones, cuando t tiende a infinito, a la solución u_∞ del problema estacionario asociado, una vez que se supone una cierta convergencia sobre los términos del lado derecho. Damos algunas condiciones suficientes para la extinción en tiempo finito de las soluciones del problema escalar. Se demuestra, asi mismo, que, al menos bajo condiciones de simetría radial, cuando el estado estacionario no es trivial, $u_\infty \neq 0$, hay casos en los que la estabilización de la solución estacionaria requiere un tiempo infinito. Para terminar, se ofrecen algunas experiencias numéricas para la formulación escalar. En particular, algunas de esas experiencias muestran un cambio instantáneo de la topología del soporte de la solución: cuando el soporte del dato inicial está formado por dos bolas disjuntas, pero suficiente cercanas, entonces, instantáneamente, para cualquier $t > 0$, el soporte de la solución $u(\,\cdot\,, t)$ se convierte en un conjunto conexo. Algunas otras experiencias numéricas se dedican al estudio del "perfil" de la solución en su momento de extinción.

1 Introduction

Bingham fluids are materials which behave as rigid bodies at low shear stress but flow as viscous fluids at high shear stress. The name is associated to Eugene C. Bingham (1878–1945) who, for the first time, in 1916, proposed a mathematical description for this visco-plastic behavior [11]. Common examples of Bingham fluids are tooth paste and paint. The Bingham model has also been used to describe the blood flow in small vessels, such as arterioles and capillaries, where the size of the vessel diameter is comparable to the size of blood cells, see e.g. [32].

The isothermal and unsteady flow of an incompressible Bingham visco-plastic medium, during the time interval $(0, T)$, is modeled by the following system of equations (clearly of the *Navier-Stokes system* type):

$$\varrho(\partial_t \mathbf{u} + (\mathbf{u}\cdot\nabla)\mathbf{u}) = \nabla\cdot\boldsymbol{\sigma} + \mathbf{f}(t,\mathbf{x}) \qquad \text{in } (0,T)\times\widetilde{\Omega}, \tag{1}$$

$$\nabla\cdot\mathbf{u} = 0 \qquad \text{in } (0,T)\times\widetilde{\Omega}, \tag{2}$$

$$\boldsymbol{\sigma} = -p\mathbf{I} + \sqrt{2}g\frac{\mathbf{D}(\mathbf{u})}{|\mathbf{D}(\mathbf{u})|} + 2\mu\mathbf{D}(\mathbf{u}), \tag{3}$$

$$\mathbf{u}(0) = \mathbf{u}_0 \qquad (\text{with } \nabla\cdot\mathbf{u}_0 = 0). \tag{4}$$

Here $\mathbf{u}$ and p represent velocity and pressure, respectively. The positive constants ϱ, μ and g represent density, viscosity and plasticity yield of the Bingham medium, respectively. Moreover, $\mathbf{f}(t,\mathbf{x})$ is a given density of external forces, $\mathbf{D}(\mathbf{v}) = [\nabla\mathbf{v} + (\nabla\mathbf{v})^t]/2$ $(= \mathrm{D}_{ij}(\mathbf{v})_{1\le i,j\le d})$, $\forall\mathbf{v}\in(H^1(\widetilde{\Omega}))^d$, and $|\mathbf{D}(\mathbf{v})|$ is the Frobenius norm of tensor $\mathbf{D}(\mathbf{v})$, i.e.,

$$|\mathbf{D}(\mathbf{v})| = \left(\sum_{1\le i,j\le d} |\mathrm{D}_{ij}(\mathbf{v})|^2\right)^{1/2}.$$

The domain $\widetilde{\Omega}$ is an open and connected subset of $\mathbb{R}^d$ ($d = 2$ or 3 in most of the applications), $\widetilde{\Gamma}$ is the boundary of $\widetilde{\Omega}$ and $T > 0$ is arbitrary fixed (and possibly $T = +\infty$).

For simplicity, we shall consider only homogeneous Dirichlet boundary conditions, namely:

$$\mathbf{u} = \mathbf{0} \qquad \text{on } (0,T)\times\widetilde{\Gamma}. \tag{5}$$

We point out that some of our results remain true, under suitable conditions, for the case of nonhomogeneous boundary conditions

$$\mathbf{u} = \mathbf{u}_B \quad \text{on } \widetilde{\Gamma}\times(0,T), \qquad \text{with } \int_{\widetilde{\Gamma}} \mathbf{u}_B(t)\cdot\mathbf{n}\,\mathrm{d}\widetilde{\Gamma} = 0, \quad \text{a.e. on } (0,T). \tag{6}$$

where $\mathbf{n}$ is the outward unit normal vector at Γ. We have denoted (and will denote later on) by $\varphi(t)$ the function $x \to \varphi(t,x)$.

We observe that if $g = 0$, system (1)–(6) reduces to the Navier-Stokes equations modeling isothermal incompressible Newtonian viscous fluid flow. We refer to the books [18] and [19] for the modeling arguments showing the equivalence with the unilateral problem stated in terms of the plasticity yield $g > 0$. The mathematical treatment of this system was carried out in [18] and [19] (see also [7, 15, 21, 22, 24] and their references).

We shall devote section 2 of this paper to the study of problem (1)–(6) for a bounded domain $\widetilde{\Omega}$ of $\mathbb{R}^2$ (i.e. $d = 2$) and for zero Dirichlet boundary conditions, i.e. $\mathbf{u}_B = \mathbf{0}$. One of our main goals is to prove the existence of a finite extinction time T_e, i.e. a time T_e such that $\mathbf{u}(t) \equiv \mathbf{0}$ for any $t \geq T_e$ for a suitable force term $\mathbf{f}(t,\mathbf{x})$. We shall prove it by means of an energy method based on the, so called, Nirenberg-Strauss inequality

$$\|\mathbf{v}\|_{(L^2(\widetilde{\Omega}))^d} \leq \gamma \int_{\widetilde{\Omega}} |\mathbf{D}(\mathbf{v})| \, \mathrm{d}\mathbf{x}, \qquad \text{for any } \mathbf{v} \in (H_0^1(\widetilde{\Omega}))^2, \tag{7}$$

(see [30]) as well as Poincaré's inequality

$$\|\mathbf{v}\|_{(L^2(\widetilde{\Omega}))^d} \leq \frac{1}{\lambda_0} \int_{\widetilde{\Omega}} |\nabla \mathbf{v}|^2 \, \mathrm{d}\mathbf{x}, \qquad \text{for any } \mathbf{v} \in (H_0^1(\widetilde{\Omega}))^2, \tag{8}$$

where γ and λ_0 are positive constants. A curious fact is that for $d = 2$ and for scalar functions, the constant γ is, in fact, independent of $\widetilde{\Omega}$ and its smallest value is $\gamma = \sqrt{\pi}/2$ (see [31]).

Here the positive constants γ and λ_0 depend only on the bounded domain $\widetilde{\Omega}$. We shall start the section by considering the associated stationary problem

$$\varrho(\mathbf{u}_\infty \cdot \nabla)\mathbf{u}_\infty = \nabla \cdot \boldsymbol{\sigma} + \mathbf{f}_\infty(\mathbf{x}) \qquad \text{in } \widetilde{\Omega}, \tag{9}$$

$$\nabla \cdot \mathbf{u}_\infty = 0 \qquad \text{in } \widetilde{\Omega}, \tag{10}$$

$$\boldsymbol{\sigma} = -p\mathbf{I} + \sqrt{2} g \frac{\mathbf{D}(\mathbf{u}_\infty)}{|\mathbf{D}(\mathbf{u}_\infty)|} + 2\mu \mathbf{D}(\mathbf{u}_\infty), \tag{11}$$

$$\mathbf{u}_\infty = \mathbf{0} \qquad \text{on } \widetilde{\Gamma}. \tag{12}$$

Our first results shows that the force must be big enough as to produce some movement. Indeed, we shall prove that if

$$\|\mathbf{f}_\infty\|_{(L^2(\widetilde{\Omega}))^2} \leq g\gamma^{-1}$$

then, necessarily $\mathbf{u}_\infty = \mathbf{0}$. After that we shall prove that, in fact, the trivial stationary state $\mathbf{u}_\infty = \mathbf{0}$ is attained in a finite time assumed

$$\|\mathbf{f}(t)\|_{(L^2(\widetilde{\Omega}))^2} \leq F(t) \qquad \text{a.e. } t > 0,$$

with $F(t) \geq 0$ such that

$$\|\mathbf{u}_0\|_{(L^2(\widetilde{\Omega}))^2} = \frac{1}{\varrho} \int_0^{t_z} \left(\frac{g}{\gamma} - F(s) \right) \mathrm{e}^{\frac{\mu\lambda_0}{\varrho} s} \, \mathrm{d}s \tag{13}$$

for some $t_z \geq 0$ and

$$\|\mathbf{u}_0\|_{(L^2(\widetilde{\Omega}))^2} \leq \frac{1}{\varrho} \int_0^{t} \left(\frac{g}{\gamma} - F(s) \right) \mathrm{e}^{\frac{\mu\lambda_0}{\varrho} s} \, \mathrm{d}s \qquad \text{for any } t \in (t_z, +\infty). \tag{14}$$

So, in that case, there exists a *finite extinction time* T_e, i.e. $\mathbf{u}(t) \equiv \mathbf{0}$ for any $t \geq T_e$. This result improves some previous extinction time results for the case $\mathbf{f}(t) \equiv \mathbf{0}$ obtained in [9, 23, 24]. The assumptions (13) and (14) are relevant even for the limit case $\mu = 0$ and have a quite different nature with respect to some conditions arising in the study of the finite extinction time for other non-Newtonian flows (see [5, 6, 7]).

The rest of the paper is devoted to the study of the above systems for a special three-dimensional domain: the unidirectional flow of an isothermal and incompressible visco-plastic Bingham fluid in an infinitely long cylinder $\widetilde{\Omega} = \Omega \times (-\infty, +\infty)$ of (bounded) cross section $\Omega \subset \mathbb{R}^2$. We start, in Subsection 3.1 by showing that if we assume

$$\mathbf{f}(t, \mathbf{x}) = (0, 0, f(t, x_1, x_2)), \qquad \text{for a.e. } t \in (0, T), \text{ and } \mathbf{x} = (x_1, x_2, x_3) \in \Omega \times (-\infty, +\infty),$$

then the axial flow velocity $u(t, x)$, i.e., $\mathbf{u} = \{0, 0, u\}$, $x = (x_1, x_2)$ (when we assume that the fluid flows in the Ox_3-direction) satisfies the following nonlinear parabolic equation

$$\begin{cases} \varrho \partial_t u - \mu \Delta u - g \nabla \cdot \left(\dfrac{\nabla u}{|\nabla u|} \right) = C(t) + f(t, x) & \text{in } \Omega \times (0, T), \\ u = 0 & \text{on } \Gamma \times (0, T), \\ u(0) = u_0, \end{cases} \tag{15}$$

where Γ is the boundary of Ω and $C(t) = -\frac{\partial p}{\partial x_3}(t, x_3)$ is the pressure drop per unit length. Due to the peculiar geometry of the three-dimensional domain there are many ways to estimate the pressure drop (for instance by prescribing a given flux flow in each transversal section and by solving then the corresponding inverse problem). So, in the rest of the paper we shall assume that $C(t)$ is a given datum of the problem.

The existence and uniqueness of solutions to problem (15) are today well-known results (see, e.g., [18] and [19, 21, 22, 24], and also [12], among other references). We assume now that

$$\begin{cases} f(t) \to f_\infty & \text{in } L^2(\Omega), \quad \text{as } t \to +\infty, \\ C(t) \to C_\infty & \text{in } \mathbb{R}, \qquad\quad \text{as } t \to +\infty, \end{cases}$$

and prove, in Subsection 3.2, that $u(t) \to u_\infty$ in $H_0^1(\Omega)$, as $t \to +\infty$, where $u_\infty(x)$ is the (unique) solution of the associated stationary problem

$$\begin{cases} -\mu \Delta u_\infty - g \nabla \cdot \left(\dfrac{\nabla u_\infty}{|\nabla u_\infty|} \right) = C_\infty + f_\infty(x) & \text{in } \Omega, \\ u_\infty = 0 & \text{on } \Gamma. \end{cases} \tag{16}$$

We use here some ideas developed in [17] in the study of the stabilization properties for a general class of quasilinear parabolic problems.

As in the vectorial system, we prove, in Subsection 3.3 that if

$$\|C_\infty + f_\infty\|_{L^2(\Omega)} \leq \frac{2g}{\sqrt{\pi}}$$

then, necessarily $u_\infty = 0$. We also prove the finite extinction time assumed that

$$\|C(t) + f(t)\|_{L^2(\Omega)} \leq F(t)$$

with $F(t) \geq 0$ satisfying (13) and (14) with $\gamma = \sqrt{\pi}/2$.

In Subsection 3.4 we consider the case in which $\Omega = B(0, R)$, the open ball of radius R centered at the origin, and assume that $f_\infty(x)$ is a radially symmetric function. We find sufficient conditions on f_∞, R and g in order to get a nontrivial (radially symmetric) solution $u_\infty(x) > 0$ for any $x \in \Omega$. We end this subsection by proving that, under symmetric and additional conditions, the convergence $u(t) \to u_\infty$ in $H_0^1(\Omega)$ as $t \to +\infty$ takes an infinite time in the sense that $u(t) \neq u_\infty$ for any $t > 0$.

The last section, Section 4, is devoted to some numerical experiences on problem (15). We study several qualitative properties of solutions: mainly, the geometry of the support of the solutions and their profile when there is extinction in a finite time. We start by considering the question of the initial propagation of the support of the solution by means of several numerical experiences. In particular, some of those experiences exhibit an instantaneous change of topology of the support of the solution: when the support of the initial datum is formed by two disjoint balls, but closed enough, then, instantaneously, for any $t > 0$, the support of the solution $u(\,\cdot\,, t)$ becomes a connected set. Some numerical experiences are devoted, in a second part of this Section, to the study of the "profile" of the solution and its extinction time.

We end this Introduction by pointing out that problem (15) can be seen as a "viscous" perturbation of the Dirichlet problem for the total variation flow

$$\begin{cases} \dfrac{\partial u}{\partial t} = \operatorname{div}\left(\dfrac{\mathrm{D}u}{|\mathrm{D}u|}\right) & \text{in } \Omega \times (0,T), \\ u = 0 & \text{on } \Gamma \times (0,T), \\ u(0,x) = u_0(x) & \text{for } x \in \Omega, \end{cases} \tag{17}$$

by setting fluid viscosity, pressure drop and external forces equal to zero, namely $\mu = 0$ and $C(t) = f(t,x) = 0$, and by setting the ratio between fluid density and plasticity yield equal to one, namely $\varrho/g = 1$. In that case the spatial gradient of the solution is only a bounded variation measure which justifies the use of the symbol $\mathrm{D}u$ instead of ∇u. Problems related to total variation flows arise not only in continuum mechanics, but also in material science [26] and image processing [29]. Existence and uniqueness of solutions to problem (17) have been obtained in [1, 2, 25]. Solutions to system (17) also enjoy some interesting properties, such as finite extinction time (meaning that $u(t) \equiv 0$ after a finite time) and no propagation of the support of the initial datum (meaning that the support of the solution $u(t,\,\cdot\,)$ is equal to the support of the initial datum), see e.g. [3]. The connected support of the solution of problem (17) when the support of the initial datum is formed by two separated balls was studied in [10]. We point out that their fine analysis techniques can not be applied to the case of $\mu > 0$ in problem (15) and so the numerical experiences presented in this paper look relevant concerning problem (15).

2 On two-dimensional Bingham flows with a nonzero external force

We assume $d = 2$,

$$\mathbf{f} \in L^2(0,T : (L^2(\widetilde{\Omega}))^2)$$

for any $T > 0$ and

$$\mathbf{u}_0 \in \mathbf{H},$$

$\mathbf{H}$ being the closure of $\mathcal{V}$ in $(L^2(\widetilde{\Omega}))^2$ with $\mathcal{V} = \{\mathbf{w} \in (\mathcal{D}(\widetilde{\Omega}))^2, \operatorname{div} \mathbf{w} = 0\}$.

There are several equivalent notions of weak solution of system (1), (2), (3), (4), (5) which can be applied according different purposes. On one hand, the system can be formulated in terms of the following *variational inequality*

$$\mathbf{u} \in L^2(0,T : \mathbf{V}), \quad p \in L^2(0,T : L^2(\widetilde{\Omega})), \qquad \text{with } \partial_t \mathbf{u} \in L^2(0,T : \mathbf{V}'),$$

such that

$$\begin{aligned} &\varrho\,\langle \partial_t \mathbf{u}(t), \mathbf{v} - \mathbf{u}(t) \rangle_{V'V} + \varrho \int_{\widetilde{\Omega}} \big(\mathbf{u}(t)\cdot\nabla\big)\mathbf{u}(t)\cdot\big(\mathbf{v} - \mathbf{u}(t)\big)\,\mathrm{d}x \\ &\qquad + \mu \int_{\widetilde{\Omega}} \nabla\mathbf{u}(t) : \nabla\big(\mathbf{v} - \mathbf{u}(t)\big)\,\mathrm{d}x - \int_{\widetilde{\Omega}} p(t)\nabla\cdot\big(\mathbf{v} - \mathbf{u}(t)\big)\,\mathrm{d}x + g\big(j(\mathbf{v}) - j(\mathbf{u}(t))\big) \\ &\quad \geq \int_{\widetilde{\Omega}} \mathbf{f}(t)\cdot\big(\mathbf{v} - \mathbf{u}(t)\big)\,\mathrm{d}x, \qquad \forall \mathbf{v} \in \mathbf{V} \text{ and a.e. } t \in (0,T), \end{aligned}$$

and

$$\mathbf{u}(0) = \mathbf{u}_0,$$

where the space $\mathbf{V}$ is defined as the closure of $\mathcal{V}$ in $(H^1(\widetilde{\Omega}))^2$ (with $\mathcal{V} = \{\mathbf{w} \in \mathcal{D}(\widetilde{\Omega})^2, \nabla \cdot \mathbf{w} = 0\}$) and

$$j(\mathbf{v}) = \int_{\widetilde{\Omega}} |\mathbf{D}(\mathbf{v})| \,\mathrm{d}x \qquad \text{for any } \mathbf{v} \in (H^1(\widetilde{\Omega}))^2.$$

Note that this variational inequality can be formulated also in terms of the multivalued subdifferential of the convex function j as

$$\varrho\big(\partial_t \mathbf{u} + (\mathbf{u} \cdot \nabla)\mathbf{u}\big) - \mu \Delta \mathbf{u} + g \partial j(\mathbf{u}) \ni -\nabla p + \mathbf{f}(t, x),$$

in a weak form, on the space $L^2(0, T : \mathbf{H})$. Moreover, another equivalent formulation can be given by rewriting the variational inequality in terms of the equation

$$\varrho\big(\partial_t \mathbf{u} + (\mathbf{u} \cdot \nabla)\mathbf{u}\big) - \mu \Delta \mathbf{u} + g \nabla \cdot \boldsymbol{\lambda} = -\nabla p + \mathbf{f}(t, x),$$

(in a weak sense) for some tensor-valued function

$$\begin{cases} \boldsymbol{\lambda} \in (L^\infty(0, T) \times \widetilde{\Omega})^{2\times 2}, \\ \boldsymbol{\lambda} = \boldsymbol{\lambda}^t, \\ |\boldsymbol{\lambda}| \leq 1 \quad \text{and} \quad \boldsymbol{\lambda} : \mathbf{D}(\mathbf{u}) = |\mathbf{D}(\mathbf{u})| \qquad \text{a.e. in } (0, T) \times \widetilde{\Omega}, \end{cases} \tag{18}$$

(see [18, 19, 22]).

Our study starts by analyzing the associated stationary problem. The above notions of solution can be adapted to this stationary case with obvious modifications.

Proposition 1 *Let* $\mathbf{f}_\infty \in (L^2(\widetilde{\Omega}))^2$ *be such that*

$$\|\mathbf{f}_\infty\|_{(L^2(\widetilde{\Omega}))^2} \leq g\gamma^{-1},$$

where γ *is the best constant in* (7)*. Then, necessarily, the solution* $\mathbf{u}_\infty \in \mathbf{V}$ *of the stationary problem* (9)*,* (10)*,* (11) *and* (12) *satisfies that* $\mathbf{u}_\infty \equiv \mathbf{0}$*. In particular the pressure* p_∞ *satisfies*

$$\nabla p_\infty(x) = g \nabla \cdot \boldsymbol{\lambda}_\infty(x) + \mathbf{f}_\infty(x) \qquad \text{in } \widetilde{\Omega},$$

for some tensor-valued function $\boldsymbol{\lambda}_\infty \in (L^\infty(\widetilde{\Omega}))^{2\times 2}$*,* $\boldsymbol{\lambda}_\infty = \boldsymbol{\lambda}_\infty^t$*,* $|\boldsymbol{\lambda}_\infty| \leq 1$ *a.e. in* $\widetilde{\Omega}$*.*

PROOF. We take as test function $\mathbf{v} = \mathbf{0}$ and $\mathbf{v} = 2\mathbf{u}_\infty$ in the associated stationary variational inequality. By adding the resulting inequalities, we get that

$$\varrho \int_{\widetilde{\Omega}} (\mathbf{u}_\infty \cdot \nabla)\mathbf{u}_\infty \cdot \mathbf{u}_\infty \,\mathrm{d}x + \mu \int_{\widetilde{\Omega}} |\nabla \mathbf{u}_\infty|^2 \,\mathrm{d}x + g j(\mathbf{u}_\infty) - \int_{\widetilde{\Omega}} p_\infty \nabla \cdot \mathbf{u}_\infty \,\mathrm{d}x = \int_{\widetilde{\Omega}} \mathbf{f}_\infty \cdot \mathbf{u}_\infty \,\mathrm{d}x.$$

But, since $\nabla \cdot \mathbf{u}_\infty = 0$ we deduce, as usual, that

$$\mu \int_{\widetilde{\Omega}} |\nabla \mathbf{u}_\infty|^2 \,\mathrm{d}x + g j(\mathbf{u}_\infty) = \int_{\widetilde{\Omega}} \mathbf{f}_\infty \cdot \mathbf{u}_\infty \,\mathrm{d}x.$$

Now, as in Proposition 6.4 of [21], we use Hölder and Nirenberg-Strauss inequality (7) to conclude that2

$$\mu \int_{\widetilde{\Omega}} |\nabla \mathbf{u}_\infty|^2 \,\mathrm{d}x + \Big(g\gamma^{-1} - \|\mathbf{f}_\infty\|_{L^2(\widetilde{\Omega})^2}\Big) \|\mathbf{u}_\infty\|_{L^2(\widetilde{\Omega})^2} \leq 0,$$

which implies the conclusion. ■

Concerning the evolution system we have the following theorem.

Theorem 1 *Let $\mathbf{f} \in L^2(0,T:(L^2(\widetilde{\Omega}))^2)$ for any $T>0$ and let $\mathbf{u}_0 \in \mathbf{H}$. Assume that*

$$\|\mathbf{f}(t)\|_{(L^2(\widetilde{\Omega}))^2} \leq F(t) \qquad \text{a.e. } t \in (0,+\infty)$$

with $F(t) \geq 0$ satisfying (13) and (14). Then, there exists a finite time $T_e \geq 0$ such that the solution $\mathbf{u}$ of the evolution problem (1), (2), (3), (4), (5) satisfies that $\mathbf{u}(t) \equiv \mathbf{0}$ for any $t \geq T_e$. In particular, for $t \geq T_e$ the pressure $p(t,x)$ satisfies that

$$\nabla p(t,x) = g\nabla \cdot \boldsymbol{\lambda}(t,x) + \mathbf{f}(t,x) \qquad \text{in } (T_e,+\infty)\times\widetilde{\Omega},$$

for some tensor-valued function $\boldsymbol{\lambda}$ satisfyng (18).

PROOF. We take as test function $\mathbf{v}=\mathbf{0}$ and $\mathbf{v}=2\mathbf{u}_\infty$ in the variational inequality. Then, by using that $\nabla\cdot\mathbf{u}=0$ and by applying Hölder, Poincaré inequality (8) and Nirenberg-Strauss inequality (7) we get, thanks to the assumptions on $\mathbf{f}(t,x)$, that

$$\frac{\varrho}{2}\frac{\mathrm{d}}{\mathrm{d}t}\|\mathbf{u}(t)\|^2_{(L^2(\widetilde{\Omega}))^2} + \mu\lambda_0\|\mathbf{u}(t)\|^2_{(L^2(\widetilde{\Omega}))^2} + g\gamma^{-1}\|\mathbf{u}(t)\|_{(L^2(\widetilde{\Omega}))^2} \leq F(t)\|\mathbf{u}(t)\|_{(L^2(\widetilde{\Omega}))^2}.$$

But, if $\|\mathbf{u}(t)\|_{(L^2(\widetilde{\Omega}))^2} > 0$ we have

$$\frac{\mathrm{d}}{\mathrm{d}t}\|\mathbf{u}(t)\|^2_{(L^2(\widetilde{\Omega}))^2} = 2\|\mathbf{u}(t)\|_{(L^2(\widetilde{\Omega}))^2}\frac{\mathrm{d}}{\mathrm{d}t}\|\mathbf{u}(t)\|_{(L^2(\widetilde{\Omega}))^2},$$

and so

$$\frac{\mathrm{d}}{\mathrm{d}t}\|\mathbf{u}(t)\|_{(L^2(\widetilde{\Omega}))^2} + \frac{\mu\lambda_0}{\varrho}\|\mathbf{u}(t)\|_{(L^2(\widetilde{\Omega}))^2} \leq \frac{1}{\varrho}F(t) - \frac{g}{\rho\gamma}.$$

Let $z(t)$ be the solution of the Cauchy problem for the linear ordinary differential equation

$$\begin{cases} z'(t) + \dfrac{\mu\lambda_0}{\varrho}z(t) = \dfrac{1}{\varrho}F(t) - \dfrac{g}{\rho\gamma} & \text{for } t>0, \\ z(0) = \|\mathbf{u}_0\|_{(L^2(\widetilde{\Omega}))^2}. \end{cases} \tag{19}$$

Then we deduce easily that

$$0 \leq \|\mathbf{u}(t)\|_{(L^2(\widetilde{\Omega}))^2} \leq z(t) \qquad \text{for any } t \in [0,T_0), \tag{20}$$

with $T_0 = \sup\left\{\tau > 0 \text{ such that } \|\mathbf{u}(t)\|_{(L^2(\widetilde{\Omega})^2)} > 0 \text{ for any } t\in[0,\tau)\right\}$. But the (unique) solution of (19) is given by the formula

$$z(t) = \mathrm{e}^{-\frac{\mu\lambda_0}{\varrho}t}\left(z(0) + \frac{1}{\varrho}\int_0^t\left(F(s) - \frac{g}{\gamma}\right)\mathrm{e}^{\frac{\mu\lambda_0}{\varrho}s}\,\mathrm{d}s\right).$$

Thus, from the assumption on $F(t)$ we know that $z(t)>0$ for any $t\in[0,t_z)$, $z(t_z)=0$ with $t_z>0$ such that

$$z(0) = \frac{1}{\varrho}\int_0^{t_z}\left(\frac{g}{\gamma} - F(s)\right)\mathrm{e}^{\frac{\mu\lambda_0}{\varrho}s}\,\mathrm{d}s$$

and $z(t) \leq 0$ for any $t\in[t_z,+\infty)$. Then, from the comparison with inequality (20) we deduce that necessarily there exists $T_e\in[0,t_z]$ such that $\|\mathbf{u}(t)\|_{(L^2(\widetilde{\Omega}))^2} = 0$ for any $t\in[T_e,+\infty)$. ∎

Remark 1 *Assumptions* (13) *and* (14) *hold trivially if*

$$\|\mathbf{f}(t)\|_{(L^2(\widetilde{\Omega}))^2} < \frac{g}{\gamma},$$

which includes the case $\mathbf{f}(t) \equiv \mathbf{0}$ *for which the finite extinction time was proved in* [22, Remark 50.4]. *Nevertheless it is not difficult to construct examples of functions* $F(t)$ *satisfying* (13) *and* (14) *but such that* $F(t) > g/\gamma$ *for many values of* $t > 0$. *Take, for instance,*

$$F(t) = \frac{g}{\gamma} + l\,\frac{\sin(t+\pi/2)}{(t+\pi/2)}$$

with $0 < l < g/\gamma$. *We also point out that assumptions* (13) *and* (14) *establish a balance, between the initial datum* $\mathbf{u}_0$ *and the forcing term* $\mathbf{f}(t)$ *leading to the finite extinction time phenomenon.*

Remark 2 *The assumptions* (13) *and* (14) *show a monotone dependence of* t_z *with respect to the plasticity yield constant* g*: the time* t_z *decreases if and only if* g *increases. Moreover the above assumptions are relevant even for the limit case* $\mu = 0$ *in which the conditions become*

$$\|\mathbf{u}_0\|_{(L^2(\widetilde{\Omega}))^2} = \frac{1}{\varrho}\int_0^{t_z}\left(\frac{g}{\gamma} - F(s)\right)\mathrm{d}s$$

for some $t_z \geq 0$ *and*

$$\|\mathbf{u}_0\|_{(L^2(\widetilde{\Omega}))^2} \leq \frac{1}{\varrho}\int_0^{t}\left(\frac{g}{\gamma} - F(s)\right)\mathrm{d}s \qquad \text{for any } t \in (t_z, +\infty).$$

Remark 3 *The assumptions* (13) *and* (14) *have a quite different nature with respect to some conditions arising in the study of the finite extinction time for other non-Newtonian flows in which the constitutive law* (3) *is replaced by*

$$\boldsymbol{\sigma} = -p\mathbf{I} + \mathbf{F}(\mathbf{D}(\mathbf{u})) + 2\mu\mathbf{D}(\mathbf{u})$$

with

$$\delta\,|\mathbf{D}(\mathbf{u})|^q \leq \mathbf{F}(\mathbf{D}(\mathbf{u})) : \mathbf{D}(\mathbf{u})$$

for some $\delta > 0$ *and some* $q \geq 1$. *The extinction in finite time was proved in* [5, 6] *and* [7] *under the assumption*

$$q \in \left(\frac{2d}{d+2}, 2\right)$$

and when

$$\|\mathbf{f}(t)\|^{q^*}_{(L^{r^*}(\widetilde{\Omega}))^d} \leq C_f\left(1 - \frac{t}{t_f}\right)_+^{q/(2-q)},$$

for some r^*, q^*, C_f *and* t_f. *Note that the result does not apply to* $d = 2$.

3 The Bingham flow in and in an infinitely long cylinder

3.1 Reduction to the scalar formulation

The rest of this paper will be devoted to the study of the special case of an unidirectional flow of an isothermal and incompressible visco-plastic Bingham fluid in a three-dimensional domain given by an infinitely long cylinder $\widetilde{\Omega} = \Omega \times (-\infty, +\infty)$ of bounded cross section $\Omega \subset \mathbb{R}^2$. It is clear that the assumption of unidirectional flow needs some appropriate conditions in the structure of the applied force. So, in our case we shall assume that

$$\mathbf{f}(t,\mathbf{x}) = (0,0,f(t,x_1,x_2)), \qquad \text{for a.e. } t \in (0,T), \quad \text{and } \mathbf{x} = (x_1,x_2,x_3) \in \Omega \times (-\infty,+\infty).$$

Then it is well known (see any classical textbook in fluid mechanics as, for instance, [8]) that the axial component flow velocity $u(t,x)$, with $x = (x_1,x_2)$, characterizes the vectorial velocity, i.e., $\mathbf{u} = (0,0,u)$. In that case, the two first components of the conservation of the momenta imply that

$$\frac{\partial p}{\partial x_1}(t,\mathbf{x}) = \frac{\partial p}{\partial x_2}(t,\mathbf{x}) = 0$$

and the third component is reduced to the nonlinear parabolic equation given in (15) with

$$C(t) = -\frac{\partial p}{\partial x_3}(t,x_3)$$

(the pressure drop per unit length). In the rest of the paper we shall assume that $C(t)$ is a given datum of the problem.

3.2 On the stabilization of solutions

We assume given

$$f \in L^2(0,T:L^2(\Omega)), \quad C \in L^2(0,T) \qquad \text{for any } T>0,$$

and

$$u_0 \in L^2(\Omega).$$

As in the precedent section, there are several equivalent notions of weak solution of problem (15) which can be applied according different purposes. On one hand, the problem can be formulated in terms of the following *variational inequality*

$$u \in C([0,+\infty):L^2(\Omega)) \cap L^2(0,T:H_0^1(\Omega)), \qquad \text{with } \partial_t u \in L^2(0,T:H^{-1}(\Omega)) \text{ for any } T>0,$$

such that

$$\begin{aligned} &\varrho\big\langle \partial_t u(t), v-u(t)\big\rangle_{H_0^1(\Omega)H^{-1}(\Omega)} + \mu\int_\Omega \nabla u(t)\cdot\nabla\big(v-u(t)\big)\,\mathrm{d}x + g\big(j(v)-j(u(t))\big) \\ &\qquad \geq \int_\Omega \big(C(t)+f(t)\big)\big(v-u(t)\big)\,\mathrm{d}x, \qquad \forall v \in H_0^1(\Omega) \text{ and a.e. } t\in(0,T), \end{aligned}$$

and

$$u(0) = u_0, \qquad \text{in } L^2(\Omega),$$

where

$$j(v) = \int_\Omega |\nabla v|\,\mathrm{d}x, \qquad \text{for any } v \in H_0^1(\Omega).$$

Note that this variational inequality can be formulated also in terms of the multivalued subdifferential of the convex function φ as

$$\varrho\,\frac{\mathrm{d}u}{\mathrm{d}t} + \partial\varphi(u) \ni C(t) + f(t) \tag{21}$$

in the Hilbert space $H = L^2(\Omega)$, with

$$\varphi(v) = \begin{cases} \dfrac{\mu}{2}\displaystyle\int_\Omega |\nabla v|^2\,\mathrm{d}x + g\int_\Omega |\nabla v|\,\mathrm{d}x & \text{if } v \in H_0^1(\Omega), \\ +\infty & \text{otherwise,} \end{cases} \tag{22}$$

(see, e.g., [12]). Moreover, another equivalent formulation can be given by rewriting the variational inequality in terms of the equation

$$\varrho\,\partial_t u - \mu\Delta u + g\nabla\cdot\boldsymbol{\lambda} = C(t) + f(t,x),$$

(in a weak sense) for some vector-valued function $\boldsymbol{\lambda} \in (L^\infty((0,T)\times\Omega))^2$,

$$|\boldsymbol{\lambda}| \le 1 \quad \text{and} \quad \boldsymbol{\lambda}\cdot\nabla u = |\nabla u| \qquad \text{a.e. in } (0,T)\times\Omega, \tag{23}$$

(see [18, 19, 22]).

We also consider the associate stationary problem (16)

$$\begin{cases} -\mu\,\Delta u_\infty - g\nabla\cdot\left(\dfrac{\nabla u_\infty}{|\nabla u_\infty|}\right) = C_\infty + f_\infty(x) & \text{in } \Omega, \\ u_\infty = 0 & \text{on } \Gamma. \end{cases}$$

Concerning the stabilization of solutions, as $t\to+\infty$, we have

Theorem 2 *Assume*

$$f \in W^{1,1}_{\text{loc}}(0,+\infty : L^2(\Omega)), \quad C \in W^{1,1}_{\text{loc}}(0,+\infty), \tag{24}$$

with

$$\int_t^{t+1} \left(|C'(s)| + \|\partial_t f(s)\|_{L^2(\Omega)}\right) \mathrm{d}s \le M, \qquad \textit{for any } t > 0,$$

for some positive constant M and let

$$u_0 \in H^1_0(\Omega)\cap H^2(\Omega).$$

Then the weak solution u of (15) *satisfies that*

$$u \in L^\infty(0,+\infty : H^1_0(\Omega)) \quad \textit{and} \quad \partial_t u \in L^2(0,+\infty : L^2(\Omega)).$$

Moreover, if there exists $C_\infty\in\mathbb{R}$ and $f_\infty \in L^2(\Omega)$ such that

$$\int_t^{t+1} \left(|C(s) - C_\infty|^2 + \|f(s) - f_\infty\|^2_{L^2(\Omega)}\right) \mathrm{d}s \to 0, \qquad \textit{as } t\to+\infty, \tag{25}$$

then $u(t)\to u_\infty$ in $H^1_0(\Omega)$ as $t\to+\infty$, where u_∞ is the unique solution of problem (16).

PROOF. We shall apply several results obtained in [17] for the stabilization properties for a general class of quasilinear parabolic problems. According [12] we know that $u_0 \in D(\partial\varphi)$. Then, by Theorem 3.6 and Lemma 3.3. of [13] we get that $u(t) \in H^1_0(\Omega)\cap H^2(\Omega)$ for a.e. $t\in(0,T)$, $\varphi(u)\in W^{1,1}(0,T)$ and $\partial_t u \in L^2(0,T : L^2(\Omega))$ for any $T>0$. To prove that $u\in L^\infty(0,+\infty : H^1_0(\Omega))$ we start by proving that the norm of u in the space $L^2(t,t+1 : H^1_0(\Omega))$ is bounded independently of t. We multiply (21) by u and integrate in $(t,t+1)\times\Omega$. Then, by Young's inequality

$$\begin{aligned} \frac{\rho}{2}\int_\Omega |u(t+1)|^2\,\mathrm{d}x - \frac{\rho}{2}\int_\Omega |u(t)|^2\,\mathrm{d}x + \mu\int_t^{t+1}\int_\Omega |\nabla u(s)|^2\,\mathrm{d}x\,\mathrm{d}s + g\int_t^{t+1}\int_\Omega |\nabla u(s)|\,\mathrm{d}x\,\mathrm{d}s \\ = \int_t^{t+1}\int_\Omega (C(s)+f(s))u(s)\,\mathrm{d}x\,\mathrm{d}s \\ \le C_\epsilon \int_t^{t+1}\int_\Omega (C(s)+f(s))^2\,\mathrm{d}x\,\mathrm{d}s + \varepsilon\int_t^{t+1}\int_\Omega |u(s)|^2\,\mathrm{d}x\,\mathrm{d}s \end{aligned}$$

for any $\varepsilon > 0$ and some $C_\epsilon > 0$. Then, by Poincaré's inquality and assumption (25) we conclude that

$$\|u\|_{L^2(t,t+1:H_0^1(\Omega))} \leq K_0$$

with K_0 independent on t. In a second step, we multiply the equation (21) by $\partial_t u$ and integrate in $(t, t+1) \times \Omega$. Then, by Lemma 3.3 of [13]

$$\begin{aligned} \rho \int_t^{t+1} \int_\Omega |\partial_t u(s)|^2 \, \mathrm{d}x \, \mathrm{d}s + \frac{\mu}{2} \int_\Omega |\nabla u(t+1)|^2 \, \mathrm{d}x + g \int_\Omega |\nabla u(t+1)| \, \mathrm{d}x \\ = \int_t^{t+1} \int_\Omega \big(C(s) + f(s)\big) \partial_t u(s) \, \mathrm{d}x \, \mathrm{d}s + \frac{\mu}{2} \int_\Omega |\nabla u(t)|^2 \, \mathrm{d}x + g \int_\Omega |\nabla u(t)| \, \mathrm{d}x \end{aligned} \tag{26}$$

But, thanks to the regularity assumption (24), a simple integration by parts shows that

$$\begin{aligned} \int_t^{t+1} \int_\Omega \big(C(s) + f(s)\big) \partial_t u(s) \, \mathrm{d}x \, \mathrm{d}s = \int_\Omega \big(C(t+1) + f(t+1)\big) u(t+1) \, \mathrm{d}x \\ - \int_\Omega \big(C(t) + f(t)\big) u(t) \, \mathrm{d}x - \int_t^{t+1} \int_\Omega \big(C'(s) + \partial_t f(s)\big) u(s) \, \mathrm{d}x \, \mathrm{d}s, \end{aligned}$$

and so, from Young's inequality and the precedent step, we conclude that

$$\|\partial_t u\|_{L^2(t,t+1:L^2(\Omega))} \leq K_1,$$

for some K_1 independent on t. Now we recall an useful technical lemma

Lemma 1 ([28]) *Let $\Phi(t) \geq 0$ be a locally bounded function such that*

$$\Phi(t+1) \leq K[\Phi(t) - \Phi(t+1)] + \theta(t),$$

where K is a positive constant and $\theta(t) \geq 0$ when t is large enough. Assume that $\theta(t) = O(1)$ as $t \to +\infty$. Then $\Phi(t) = O(1)$ as $t \to +\infty$.

By applying Lemma 1 to

$$\Phi(t) = \frac{\mu}{2} \int_\Omega |\nabla u(t+1)|^2 \, \mathrm{d}x + g \int_\Omega |\nabla u(t+1)| \, \mathrm{d}x$$

and $\theta(t)$ a suitable positive constant we get that $u \in L^\infty(0, +\infty : H_0^1(\Omega))$. As a consequence, from (26) we get that $\partial_t u \in L^2(0, +\infty : L^2(\Omega))$. Now we are in conditions to apply Theorem 1 of [17] which implies that the *omega limit set*

$$\omega(u) = \big\{u_\infty \in H_0^1(\Omega) : \exists\, t_n \to +\infty \text{ such that } u(t_n) \to u_\infty \text{ in } L^2(\Omega)\big\}$$

is not empty and that, in fact, it is formed by solutions of the stationary problem (16). Moreover, since this problems only admits a unique solution we deduce the convergence in $L^2(\Omega)$ of any $t_n \to +\infty$, i.e. $u(t) \to u_\infty$ in $L^2(\Omega)$ as $t \to +\infty$. Finally, since the operator $u \longmapsto \partial\varphi(u)$ is coercive in $H_0^1(\Omega)$, in the sense that

$$\int_\Omega \big(\partial\varphi(u) - \partial\varphi(v)\big)(u - v) \, \mathrm{d}x = \mu \int_\Omega |\nabla(u - v)|^2 \, \mathrm{d}x + g \int_\Omega |\nabla(u - v)| \, \mathrm{d}x \geq \mu \int_\Omega |\nabla(u - v)|^2 \, \mathrm{d}x,$$

we deduce that the convergence $u(t) \to u_\infty$, as $t \to +\infty$, takes place, in fact, in $H_0^1(\Omega)$ (see Theorem 2 of [17]). ■

3.3 On the finite extinction time for the scalar formulation

The results of Section 1 for the vectorial formulation admit an automatic replica for the case of the scalar problem (15), where now the role of ∇p is replaced by the spatially constant function $C(t)$ and γ takes the value $\gamma = \sqrt{\pi}/2$. So, concerning the stationary problem (16) we have:

Proposition 2 *Let $f_\infty \in L^2(\Omega)$ be such that*

$$\|C_\infty + f_\infty\|_{L^2(\Omega)} \leq \frac{2g}{\sqrt{\pi}}.$$

Then, necessarily, the solution $u_\infty \in H_0^1(\Omega)$ of the stationary problem (16) satisfies that $u_\infty \equiv 0$. In particular

$$-g\nabla \cdot \boldsymbol{\lambda}_\infty(x) = C_\infty + f_\infty(x) \qquad \text{in } \widetilde{\Omega},$$

for some vector-valued function $\boldsymbol{\lambda}_\infty \in (L^\infty(\Omega))^2$, $|\boldsymbol{\lambda}_\infty| \leq 1$ a.e. in Ω.

With respect to the finite extinction time we have

Theorem 3 *Let $f \in L^2(0,T : L^2(\Omega))$, $C \in L^2(0,T)$ for any $T > 0$ and let $u_0 \in L^2(\Omega)$. Assume that*

$$\|C(t) + f(t)\|_{L^2(\Omega)} \leq F(t) \qquad \text{a.e. } t \in (0,+\infty)$$

with $F(t) \geq 0$ satisfying (13) and (14) with $\gamma = \sqrt{\pi}/2$. Then, there exists a finite time $T_e \geq 0$ such that the solution u of the evolution problem (15) satisfies that $u(t) \equiv 0$ for any $t \geq T_e$. In particular, for $t \geq T_e$ we have

$$-g\nabla \cdot \boldsymbol{\lambda}(t,x) = C(t) + f(t,x) \qquad \text{in } (T_e,+\infty) \times \widetilde{\Omega},$$

for some tensor-valued function $\boldsymbol{\lambda}$ satisfying (23).

The proof is an obvious adaptation of the of the proof of Theorem 1. We emphasize that Remarks 1, 2 and 3 have some interest also for the scalar case. We point out that the limit case $\mu = 0$ corresponds to the non-homogeneous problem associated to the total variation flow (17).

3.4 On the stationary symmetric formulation and the stabilization of solutions in an infinite time

In this Subsection we shall consider only the radially symmetric case in which $\Omega = B(0,R)$, the open ball of radius R centered at the origin, and the data of the problem are assumed to be radially symmetric and nonnegative functions.

We start by studying the stationary problem (16). The uniqueness of solutions implies that the problem can be formulated in the following terms: given

$$C_\infty > 0,\ f_\infty \geq 0 \quad \text{with} \int_0^R f_\infty(r)^2 r\,\mathrm{d}r < +\infty, \tag{27}$$

find $u_\infty \in H_0^1(B(0,R))$ such that

$$\begin{cases} -\dfrac{\mu}{r}\dfrac{\mathrm{d}}{\mathrm{d}r}\left(r\dfrac{\mathrm{d}u_\infty}{\mathrm{d}r}(r)\right) - \dfrac{g}{r}\dfrac{\mathrm{d}}{\mathrm{d}r}\big(r\lambda_\infty(r)\big) = C_\infty + f_\infty(r), & \text{for } r \in (0,R), \\ u_\infty(R) = 0 & \text{and} \\ \dfrac{\mathrm{d}u_\infty}{\mathrm{d}r}(0) = 0, \end{cases} \tag{28}$$

for some scalar-valued function $\lambda_\infty \in L^\infty(0,R)$ satisfying

$$|\lambda_\infty(r)| \le 1 \quad \text{and} \quad \lambda_\infty(r)\frac{\mathrm{d}u_\infty}{\mathrm{d}r}(r) = \left|\frac{\mathrm{d}u_\infty}{\mathrm{d}r}(r)\right| \qquad \text{a.e. in } (0,R). \tag{29}$$

Note that, by the regularity proved in [12], we know that $u_\infty \in H^2(B(0,R))$. In fact, this implies that $u_\infty \in C^1([0,R))$ and that $r\lambda_\infty(r)$ is an element of $H^1(B(0,R))$ and, that, in particular, $\lambda_\infty \in C^0(0,R)$. We also mention that condition (29) can be equivalently written as

$$\lambda_\infty(r) \in \operatorname{sign}\left(\frac{\mathrm{d}u_\infty}{\mathrm{d}r}(r)\right) \qquad \text{a.e. in } (0,R),$$

where sign denotes the maximal monotone graph of $\mathbb{R}^2$ given by $\operatorname{sign}(s) = +1$ if $s > 0$, $\operatorname{sign}(s) = -1$ if $s < 0$ and $\operatorname{sign}(0) = [-1,+1]$.

We are interested in finding some sufficient conditions on C_∞, f_∞, R, μ and g in order to get a nontrivial (radially symmetric) solution $u_\infty(r) > 0$ for any $r \in (0,R)$. To simplify the exposition we shall consider only the case in which the *solid region* generated by the solution, $S(u_\infty) = \{r \in [0,R) : \frac{\mathrm{d}u_\infty}{\mathrm{d}r}(r) = 0\}$, is a connected set. As we shall see, in our case it is related to the monotonicity of the function $\lambda_\infty(r)$. In order to get this property we shall assume a slightly technical additional condition on $f_\infty(r)$:

$$r\big(C_\infty + f_\infty(r)\big) > \int_0^r s\big(C_\infty + f_\infty(s)\big)\,\mathrm{d}s \qquad \text{for any } r \in (0,R). \tag{30}$$

It is easy to check that condition (30) is trivially satisfied if, for instance, $f_\infty(r) \equiv 0$ and that it also holds for some concave profiles of $f_\infty(r)$ as, for instance, $f_\infty(r) = \omega(R - r^2)$ under suitable conditions on ω and R in terms of a given C_∞.

We have

Proposition 3 *Assume C_∞ and f_∞ satisfying (27) and (30). Then:*

a) if

$$\frac{1}{gR}\int_0^R s\big(C_\infty + f_\infty(s)\big)\,\mathrm{d}s < 1 \tag{31}$$

the solution $u_\infty(r)$ of (28) is the trivial solution $u_\infty(r) \equiv 0$ and $\lambda_\infty(r)$ is the decreasing function given by

$$\lambda_\infty(r) = -\frac{1}{gr}\int_0^r s\big(C_\infty + f_\infty(s)\big)\,\mathrm{d}s, \qquad \textit{for any } r \in (0,R],$$

b) if we assume that there exists a $R_0 \in (0,R)$ such that

$$\frac{1}{gR_0}\int_0^{R_0} s\big(C_\infty + f_\infty(s)\big)\,\mathrm{d}s = 1, \tag{32}$$

then $u_\infty(r)$ is given by

$$u_\infty(r) = \begin{cases} \displaystyle\int_{R_0}^R \left(\frac{1}{\mu\sigma}\int_0^\sigma s\big(C_\infty + f_\infty(s)\big)\,\mathrm{d}s - \frac{g}{\mu}\right)\mathrm{d}\sigma & \textit{if } r \in (0,R_0), \\ \displaystyle\int_r^R \left(\frac{1}{\mu\sigma}\int_0^\sigma s\big(C_\infty + f_\infty(s)\big)\,\mathrm{d}s - \frac{g}{\mu}\right)\mathrm{d}\sigma & \textit{if } r \in (R_0,R), \end{cases}$$

and $\lambda_\infty(r)$ is given by the nondecrasing function

$$\lambda_\infty(r) = \max\left\{-\frac{1}{gr}\int_0^r s\big(C_\infty + f_\infty(s)\big)\,\mathrm{d}s,\ -1\right\} \qquad \textit{for any } r \in (0,R].$$

PROOF. We introduce the function

$$\psi(r) = \frac{1}{gr}\int_0^r s\big(C_\infty + f_\infty(s)\big)\,\mathrm{d}s.$$

Then, by differentiation we see that condition (30) implies that $\psi(r)$ is a strictly increasing function. Moreover, by l'Hôpital rule, $\psi(0) = 0$, so $\psi(r) > 0$ for any $r \in (0, R]$. On any positively measured subset of the solid region $S(u_\infty)$ the equation reduces to the condition

$$-\frac{g}{r}\frac{\mathrm{d}}{\mathrm{d}r}\big(r\lambda_\infty(r)\big) = C_\infty + f_\infty(r).$$

But, as $\frac{\mathrm{d}u_\infty}{\mathrm{d}r}(0) = 0$, if we denote by R_0 (with $R_0 \in (0, R]$) to the boundary of the first connected component of $S(u_\infty)$, we get that necessarily

$$\lambda_\infty(r) = -\psi(r) = -\frac{1}{gr}\int_0^r s\big(C_\infty + f_\infty(s)\big)\,\mathrm{d}s \qquad \text{for any } r \in [0, R_0]. \tag{33}$$

Now, to prove a) it suffices to use the fact that $\psi(r)$ is a strictly increasing function and that condition (31) implies that $\lambda_\infty(R) = -\psi(R) \in (-1, 0)$. Thus, $\lambda_\infty(r) \in \mathrm{sign}(0)$ a.e. in $(0, R)$ and the choice $u_\infty(r) \equiv 0$ satisfies all the requirements as to be a solution of problem (28). Moreover, by the uniqueness of solutions, $u_\infty(r) \equiv 0$ is the unique choice satisfying all the conditions of weak solution of (28).
In the case b) the expression (33) and the facts that $\psi(r)$ is a strictly increasing function and that we must have $|\lambda_\infty(r)| \le 1$ for any $r \in [0, R]$ imply that, necessarily, $\lambda_\infty(r) = -1$ for any $r \in [R_0, R]$. Note that the continuity of function $\lambda_\infty(r)$ is assured thanks to the condition (32). Finally, once that we have determined function $\lambda_\infty(r)$ on $[0, R]$ the (unique) expression for $u_\infty(r)$ can be found by integrating twice in the equation

$$\frac{\mathrm{d}}{\mathrm{d}r}\left(r\frac{\mathrm{d}u_\infty}{\mathrm{d}r}(r)\right) = \frac{r}{\mu}\left(-\frac{g}{r}\frac{\mathrm{d}}{\mathrm{d}r}(r\lambda_\infty(r)) - C_\infty + f_\infty(r)\right),$$

and using the fact that $u_\infty(R) = 0$ and $\frac{\mathrm{d}u_\infty}{\mathrm{d}r}(r) = 0$ for any $r \in [0, R_0]$. ■

Remark 4 *The above result gives a necessary and sufficient condition in order to have a trivial solution $u_\infty(r) \equiv 0$ of problem (28), once we assume the technical additional condition (30). Obviously, this is sharper than the general sufficient condition given in Proposition 2 for a general class of functions f (not necessarily radially symmetric). Note also that condition (31) is stated in terms of the L^1 norm of function $f(r)$ and that it is independent of μ. In fact the above characterization remains true for the limit case $\mu = 0$ but in this case, as in the paper ([3]), the solution u_∞ must be searched in the class of bounded variation functions. We also point out that the technical condition (30) is equivalent to the monotonicity of function $\lambda_\infty(r)$. For instance, a solution with a solid region $S(u_\infty)$ with more than one connected components can not be associated, in general, to a monotone function $\lambda_\infty(r)$.*

Remark 5 *If $f_\infty \equiv 0$ it is a routine matter to check that the above statement leads to the explicit solution mentioned in the references [21, 22, 24],*

$$u_\infty(r) = \begin{cases} \left(\dfrac{R-R_0}{2\mu}\right)\left(\dfrac{C_\infty}{2}(R+R_0) - 2g\right) & \text{if } r \in (0, R_0), \\[2ex] \left(\dfrac{R-r}{2\mu}\right)\left(\dfrac{C_\infty}{2}(R+r) - 2g\right) & \text{if } r \in (R_0, R). \end{cases}$$

Other properties of the solid region $S(u_\infty)$ (and its complementary: $\Omega^+ = \Omega - S(u_\infty)$) can be found in [27]. For the application of rearrangement techniques (leading to some estimates on the measure of the solid region in non symmetric domains) see the exposition made in ([16]).

We consider now the parabolic problem (15) for radially symmetric data and $\Omega = B(0,R)$. Our purpose is to find some sufficient conditions ensuring that when the solution u_∞ of the associate stationary problem is not trivial then convergence $u(t) \to u_\infty$ in $H_0^1(\Omega)$, as $t \to +\infty$, takes an infinite time in the sense that $u(t) \neq u_\infty$ for any $t > 0$. To simplify the exposition we consider an autonomous right hand side term. So, given C_∞ and f_∞ satisfying (27) and (30), and given

$$u_0 \in H_0^1(B(0,R)) \cap H^2(B(0,R)) \qquad \text{with } u_0(r) \geq 0, r \in (0,R), \tag{34}$$

our problem is to find $u \in L^\infty(0,+\infty : H_0^1(B(0,R))$ such that

$$\begin{cases} \varrho \dfrac{\partial u}{\partial t}(t,r) - \dfrac{\mu}{r}\dfrac{\partial}{\partial r}\left(r\dfrac{\partial u}{\partial r}(t,r)\right) - \dfrac{g}{r}\dfrac{\partial}{\partial r}\big(r\lambda(t,r)\big) = C_\infty + f_\infty(r), & \text{for } t \in (0,+\infty),\ r \in (0,R), \\ u(t,R) = 0 \quad \text{and} \quad \dfrac{\partial u}{\partial r}(t,0) = 0, & \text{for } t \in (0,+\infty), \\ u(0,r) = u_0(r) & r \in (0,R), \end{cases} \tag{35}$$

for some scalar-valued function $\lambda \in L^\infty((0,+\infty) \times B(0,R))$ satisfying

$$|\lambda(t,r)| \leq 1 \quad \text{and} \quad \lambda(t,r)\frac{\partial u}{\partial r}(t,r) = \left|\frac{\partial u}{\partial r}(t,r)\right| \qquad \text{a.e. } r \in (0,R), \text{ for a.e. } t \in (0,+\infty).$$

Thanks to the stabilization result of Subsection 3.2, we know that the weak solution u of (35) satisfies that

$$u \in L^\infty(0,+\infty : H_0^1(B(0,R))) \quad \text{and} \quad \partial_t u \in L^2(0,+\infty : L^2(B(0,R))).$$

and that $u(t) \to u_\infty$ in $H_0^1(B(0,R))$ as $t \to +\infty$, where u_∞ is the unique solution of problem (28). Moreover, by applying the abstract theory for subdifferential operators ([13]) and the fact that $D(\partial\varphi) = H_0^1(B(0,R)) \cap H^2(B(0,R))$ we also know that

$$u \in L^2(0,+\infty : H_0^1(B(0,R)) \cap H^2(B(0,R))).$$

As in the stationary case, this implies that $u(t) \in C^1([0,R))$ and that $r\lambda(t,r)$ is an element of $H^1(B(0,R))$ and, that, in particular, $\lambda(t) \in C^0(0,R)$, for a.e. $t > 0$.

By Proposition 3 we know that u_∞ is not trivial ($u_\infty \neq 0$) if we assume condition (32).

Theorem 4 *Let C_∞, f_∞ and u_0 satisfying (27), (30), (34) and (32). Then, there exits a $R^* \in (0,R)$ such that*

$$\|u(t) - u_\infty\|_{C^0([R^*,R])} > 0 \qquad \textit{for any } t > 0.$$

PROOF. The convergence $u(t) \to u_\infty$ in $H_0^1(B(0,R))$ as $t \to +\infty$ proved in Theorem 2 and the symmetry of the functions imply that $u(t) \to u_\infty$ in $C^0([0,R])$ as $t \to +\infty$ and that $\lambda(t,r) \to \lambda_\infty(r)$ in $L^2(B(0,R))$ as $t \to +\infty$. By using the additional regularity $u \in L^2(0,+\infty : H_0^1(B(0,R)) \cap H^2(B(0,R)))$ and the abstract result Theorem 3.10 of [13] we get that

$$\lim_{t\to+\infty}\left\|\frac{\partial u}{\partial t}(t)\right\|_{L^2(B(0,R))} = 0,$$

which, implies that

$$\lim_{t\to+\infty}\left\|\left(\frac{\mu}{r}\frac{\partial}{\partial r}\left(r\frac{\partial u}{\partial r}(t,r)\right) + \frac{g}{r}\frac{\partial}{\partial r}(r\lambda(t,r))\right) - \left(\frac{\mu}{r}\frac{\mathrm{d}}{\mathrm{d}r}\left(r\frac{\mathrm{d}u_\infty}{\mathrm{d}r}(r)\right) + \frac{g}{r}\frac{\mathrm{d}}{\mathrm{d}r}(r\lambda_\infty(r))\right)\right\|_{L^2(B(0,R))} = 0.$$

Then, by the regularity shown in [12], we have that $u(t) \to u_\infty$ in $H^2(B(0,R))$, and by the symmetry of $u(t,r)$ and $u_\infty(r)$ we get that, in fact, $u(t) \to u_\infty$ in $W_0^{1,\infty}(B(0,R))$ as $t \to +\infty$. This implies that

$\lambda(t,r) \to \lambda_\infty(r)$ in $L^\infty(B(0,R))$, and so in $C^0(B(0,R))$, as $t \to +\infty$. In particular, since $\lambda_\infty(r) = -1$ for any $r \in [R_0, R]$, we deduce that there exists a time T^*, large enough, and $R^* \in (R_0, R)$ such that $u(t,r)$ satisfies

$$\begin{cases} \varrho \dfrac{\partial u}{\partial t}(t,r) - \dfrac{\mu}{r}\dfrac{\partial}{\partial r}\left(r\dfrac{\partial u}{\partial r}(t,r)\right) = -\dfrac{g}{r} + C_\infty + f_\infty(r), & \text{for } t \in (T^*, +\infty), r \in (R^*, R), \\ u(t,R) = 0 \quad \text{and} \quad u(t,R^*) = h(t) & \text{for } t \in (T^*, +\infty), \\ u(T^*, r) = U_0(r) & r \in (R^*, R), \end{cases} \tag{36}$$

where

$$h(t) \to h_\infty \quad \text{as } t \to +\infty, \qquad \text{with } h_\infty = u_\infty(R^*),$$

and

$$U_0 \in H_0^1(B(0,R)) \cap H^2(B(0,R)).$$

Analogously, we have that

$$\begin{cases} -\dfrac{\mu}{r}\dfrac{\mathrm{d}}{\mathrm{d}r}\left(r\dfrac{\mathrm{d}u_\infty}{\mathrm{d}r}(r)\right) = -\dfrac{g}{r} + C_\infty + f_\infty(r), \quad \text{for } r \in (R^*, R), \\ u_\infty(R) = 0 \\ u_\infty(R^*) = h_\infty. \end{cases} \tag{37}$$

But, problems (36) and (37) are now linear problems and so, by the strong maximum principle or by using the integral representations of solutions (see, e.g. [20]), we know that $\|u(t) - u_\infty\|_{C^0([R^*,R])} > 0$ for any $t > 0$, which ends the proof. ■

Remark 6 *Note that the convergence $\lambda(t,r) \to \lambda_\infty(r)$ as $t \to +\infty$, in different functional spaces, is equivalent to the convergence of the free boundaries $\partial S(u(t))$ to the stationary free boundary $\partial S(u_\infty)$, as $t \to +\infty$, in different weak senses.*

4 On the numerical approach of solutions of Bingham type flows in cylinders

As mentioned in Subsection 3.2, it follows from references [18] and [19] that a mechanically and mathematically correct formulation of problem (15) is provided by the following *variational inequality type* problem in which, for simplicity, we assume $f \equiv 0$ and $C(t) \equiv C$:

$$\begin{cases} \text{Find } u \in L^2(0,T : H_0^1(\Omega)) \text{ such that} \\ \quad \varrho\langle \partial_t u, (v-u)\rangle + \mu \displaystyle\int_\Omega \nabla u \cdot \nabla(v-u)\,\mathrm{d}x + g(j(v) - j(u)) \\ \qquad \geq C \int_\Omega (v-u)\,\mathrm{d}x, \qquad \forall v \in H_0^1(\Omega), \\ \quad u(0) = u_0, \end{cases} \tag{38}$$

with

$$j(v) = \int_\Omega |\nabla v|\,\mathrm{d}x.$$

Note that, in fact, $u \in C([0,T] : L^2(\Omega))$. The backward Euler scheme, described below, is a good iterative algorithm preserving the asymptotic behavior of the solution of the continuous problem (namely, problem (38)), including the finite extinction time, see [15]. This scheme reads as follows (with Δt a positive time discretization step that we suppose constant, for simplicity): we start assuming

$$u^0 = u_0$$

and then, for $n \geq 1$, compute u^n from u^{n-1} via the solution of the stationary problem

$$\begin{cases} \text{Find } u^n \in H_0^1(\Omega), \\ \quad \varrho \displaystyle\int_\Omega (u^n - u^{n-1})(v - u^n) : \mathrm{d}x + \mu \Delta t \int_\Omega \nabla u^n \cdot \nabla (v - u^n)\, \mathrm{d}x + g\Delta t (j(v) - j(u^n)) \\ \quad \geq \Delta t C^n \int_\Omega (v - u^n) : \mathrm{d}x, \qquad \forall v \in H_0^1(\Omega), \end{cases} \tag{39}$$

with $C^n = C(n\Delta t)$. It follows from, e.g., [21, Chapter I], that (39) is an elliptic variational inequality (of the so called "second kind") problem, which has a unique solution. Problem (39) can be rewritten as

$$\begin{cases} \text{Find } u \in H_0^1(\Omega), \\ \quad \alpha \displaystyle\int_\Omega u(v - u)\, \mathrm{d}x + \mu \int_\Omega \nabla u \cdot \nabla (v - u)\, \mathrm{d}x + g(j(v) - j(u)) \\ \quad \geq \displaystyle\int_\Omega f(v - u)\, \mathrm{d}x, \qquad \forall v \in H_0^1(\Omega), \end{cases} \tag{40}$$

with $\alpha \geq 0$ and $f \in L^2(\Omega)$.

A classical method to solve problem (40) is the one introduced in reference [14]; it reduces the solution of the above problem to the solution of a sequence of linear Dirichlet problems for the operator $\alpha I - \mu\Delta$ and some simple projection operations. The method relies on the equivalence between (40) and

$$\begin{cases} \alpha u - \mu \Delta u - g \nabla \cdot \boldsymbol{\lambda} = f & \text{in } \Omega, \\ u = 0 & \text{on } \Gamma, \\ \boldsymbol{\lambda} \cdot \nabla u = |\nabla u|, & \boldsymbol{\lambda} \in \boldsymbol{\Lambda}, \end{cases} \tag{41}$$

the last two relations implying that

$$\boldsymbol{\lambda} = P_{\boldsymbol{\Lambda}}(\boldsymbol{\lambda} + rg\nabla u), \qquad \forall r \geq 0, \tag{42}$$

with the operator $P_{\boldsymbol{\Lambda}}$ defined by

$$P_{\boldsymbol{\Lambda}}(\mathbf{q})(x) = \frac{\mathbf{q}(x)}{\max(1, |\mathbf{q}(x)|)}, \qquad \text{a.e. on } \Omega, \forall \mathbf{q} \in (L^2(\Omega))^N.$$

Here $\boldsymbol{\Lambda} = \{\mathbf{w} \in L^\infty(\Omega)^N : |\mathbf{w}(x)| \leq 1 \text{ a.e. } x \in \Omega\}$ and $N = d \times d$.

In order to solve (40), via relation (41) and (42), we advocate (following [14]) the fixed point algorithm below:

$$\boldsymbol{\lambda}^0 \text{ is given in } \boldsymbol{\Lambda} \tag{43}$$

then, for $n \geq 0$, assuming that λ^n is known, we compute u^n and then λ^{n+1} as follows: solve

$$\alpha u^n - \mu \Delta u^n = f + g \nabla \cdot \boldsymbol{\lambda}^n \quad \text{in } \Omega, \qquad u^n = 0 \quad \text{on } \Gamma, \tag{44}$$

and

$$\boldsymbol{\lambda}^{n+1} = P_{\boldsymbol{\Lambda}}\big(\boldsymbol{\lambda}^n + rg\nabla u^n\big). \tag{45}$$

Suppose that the system (41) has a solution $\{u, \lambda\} \in H_0^1(\Omega) \times \boldsymbol{\Lambda}$ (which is indeed the case); it can be shown (see, e.g., refs. [21] and [24]) that the above pair is necessarily a saddle-point over $H_0^1(\Omega) \times \boldsymbol{\Lambda}$ of the Lagrangian functional

$$\mathcal{L} : H^1(\Omega) \times (L^2(\Omega))^N \to \mathbb{R}$$

defined by

$$\mathcal{L}(v,\boldsymbol{\mu}) = \frac{1}{2}\left[\alpha\|v\|^2_{L^2(\Omega)} + \mu\|\nabla v\|^2_{(L^2(\Omega))^2}\right] + g\int_\Omega \boldsymbol{\mu}\cdot\nabla v\,\mathrm{d}x - \int_\Omega f v\,\mathrm{d}x \tag{46}$$

i.e., the pair $\{u,\boldsymbol{\lambda}\}$ verifies (from the definition of a saddle-point; see, e.g., [22, Chapter 4])

$$\begin{cases} \{u,\boldsymbol{\lambda}\} \in H^1_0(\Omega)\times\boldsymbol{\Lambda}, \\ \mathcal{L}(u,\boldsymbol{\mu}) \le \mathcal{L}(u,\boldsymbol{\lambda}) \le \mathcal{L}(v,\boldsymbol{\lambda}), \quad \forall\{v,\boldsymbol{\mu}\}\in H^1_0(\Omega)\times\boldsymbol{\Lambda}. \end{cases} \tag{47}$$

Conversely, any solution of (47) is solution of system (41). It follows from the above reference that algorithm (43)–(45) is nothing but an Uzawa algorithm applied to the solution of the saddle-point problem (47) with L defined by (46); for a systematic study of Uzawa algorithms, see, e.g., [22, Chapter 4], and the references therein.

4.1 Some numerical experiments

In this section we present some numerical results related to problem (15), most of them for $C = 0$ and $f = 0$, with the goal of investigating the qualitative properties (i.e. finite extinction time and propagation of support of initial data) of solutions to the Bingham flow in a cylinder.

In all our simulations, the spatial domain is chosen to be the unit square in $\mathbb{R}^2$, namely $\Omega = (0,1)\times(0,1)$ [m×m]. The fluid density and plasticity yield are chosen to be $\rho = 1$ [Kg m^{-3}] and $g = 2$ [Pa]. For what concerns the fluid viscosity, we run simulations with $\mu = 0.25$ and $\mu = 0.0025$ [Pa s], in order to investigate how the fluid viscosity affects the dynamics of the flow. Moreover, we assume the pressure drop to be equal to zero, namely $C = 0$ [Pa m^{-1}], so that the flow is driven only by the initial conditions. These choices are summarized in Table 1.

Fluid domain	Ω =$(0,1)\times(0,1)$ [m×m]
Fluid density	ρ=1 [Kg m^{-3}]
Plasticity yield	g=2 [Pa]
Fluid viscosity	$\mu = 0.25, 0.0025$ [Pa s]
Pressure drop	$C = 0$ [Pa m^{-1}]

Table 1. Values of the parameters used in the numerical simulations.

We are going to consider a set of five different initial conditions:

Case I - Characteristic function of a disk. The initial velocity u_0 is given by:

$$u_0 = \begin{cases} 1 & \text{in } B(x_0,R_1) \\ 0 & \text{elsewhere} \end{cases}$$

with $x_0 = (0.5, 0.5)$ and $R_1 = 0.3$.

Case II - Superposition of two characteristic functions. The initial velocity u_0 is given by:

$$u_0 = \begin{cases} 2 & \text{in } B(x_0,R_2) \\ 1 & \text{in } B(x_0,R_1)\setminus B(x_0,R_2) \\ 0 & \text{elsewhere} \end{cases}$$

with $x_0 = (0.5, 0.5)$, $R_1 = 0.3$, and $R_2 = 0.2$.

Case III - Characteristic function of two (distant) disjoint disks. The initial velocity u_0 is given by:

$$u_0 = \begin{cases} 1 & \text{in } B(x_1, R_1) \cup B(x_2, R_2) \\ 0 & \text{elsewhere} \end{cases}$$

with $x_1 = (0.2750, 0.2750)$, $x_2 = (0.7250, 0.7250)$, and $R_1 = R_2 = 0.1$.

Case IV - Characteristic function of two (close) disjoint disks. The initial velocity u_0 is given by:

$$u_0 = \begin{cases} 1 & \text{in } B(x_1, R_1) \cup B(x_2, R_2) \\ 0 & \text{elsewhere} \end{cases}$$

with $x_1 = (0.4242, 0.4242)$, $x_2 = (0.5758, 0.5758)$, and $R_1 = R_2 = 0.1$.

Case V - Characteristic function of a square. The initial velocity u_0 is given by:

$$u_0 = \begin{cases} 1 & \text{in } S = (a, b) \times (a, b) \\ 0 & \text{elsewhere} \end{cases}$$

with $a = 0.25$ and $b = 0.75$.

Case VI - Non zero value of C. The initial velocity u_0 is given by:

$$u_0 = \begin{cases} 1 & \text{in } B(x_0, R_1) \\ 0 & \text{elsewhere} \end{cases}$$

with $x_0 = (0.5, 0.5)$ and $R_1 = 0.3$. The value of C is varied in a range from 1 to 8

4.2 Numerical results

Problem (15) was solved using the iterative method á la Uzawa (43)–(45). We validated our results by repeating the simulations using different time steps, different mesh sizes and different tolerances for the convergence of the Uzawa algorithm. More precisely, we used $\Delta t = 10^{-4}$, 5×10^{-4}, 10^{-5} as time steps; we used $1/70$, $1/100$, $1/120$, $1/150$ as mesh sizes; we used $tol = 10^{-6}$, 5×10^{-6}, 10^{-7} as tolerances for the convergence of the Uzawa algorithm. Excellent agreement was found between results obtained with different combinations of these parameters.

Finite extinction time. Our results show a finite extinction time of the solution, as predicted by the theory (see Theorem 3). Figures 1, 6, 11, 16, 21 show the time evolution of the L^2-norm of the solution, namely $\|u\|_{L^2(\Omega)}(t)$, for each of the five different initial conditions. The pictures show that the extinction time increases as the fluid viscosity decreases, see Table 2. This is due to the fact that a less viscous system has a less efficient dissipative mechanism and therefore it takes longer for the solution to decay to zero.

	Case I	Case II	Case III	Case IV	Case V
$\mu = 0.25$ [Pa s]	0.0505	0.071	0.012	0.019	0.0465
$\mu = 0.0025$ [Pa s]	0.0705	0.1025	0.0215	0.028	0.064

Table 2. Numerically computed values of extinction times corresponding to different initial conditions (Cases I to V) and to different fluid viscosities ($\mu = 0.25$ and $\mu = 0.0025$ [Pa s].)

In particular, in Case I problem (17) (formally corresponding to problem (15) with $\mu = 0$) admits the following exact solution

$$u(t,x) = \operatorname{sign}(k)\frac{d}{r}\left(\frac{|k|r}{gd} - t\right)^{+} \chi_{B(0,r)}(x).$$

It is easy to see that $u(t,x)$ vanishes for $t = (|k|r)/(gd)$, and this represents the extinction time in the case of $\mu = 0$. For the values in Table 1, we find that $(|k|r)(gd) = 0.075$ [s]. The agreement with the extinction time obtained with our simulations is very good: we get $t = 0.0705$ for $\mu = 0.0025$ [Pa s], see Table 2. We emphasize that the theoretical value of the extinction time is obtained for the total variation flow problem, which corresponds to a Bingham fluid with no viscosity. On the other hand, our simulations include a non-zero fluid viscosity and, as a consequence, the solution extinction time is smaller than the theoretical value. As expected though, as the fluid viscosity decreases, the extinction time increases.

Solution and normalized solution. We have visualized the time evolution of the solution $u(t,x)$ and of the normalized solution $u(t,x)/\|u\|_{L^2(\Omega)}(t)$. The solution $u(t,x)$ progressively decreases to zero, while the normalized solution reaches a non-zero and non-smooth limit in a finite time. In order to better visualize the comparison between the solution and the normalized solution, we show their time-evolution restricted to the domain diagonal, see Figures 3 and 4 for Case I, Figures 8 and 9 for Case II, Figures 13 and 14 for Case III, Figures 18 and 19 for Case IV, Figures 23 and 24 for Case V. The fact that the normalized solution reaches a non-zero and non-smooth limit at the extinction time should not be a surprise. Solutions to total variation flow problems do not gain any spatial differentiability, in contrast with what happens for the linear heat equation and many other quasilinear parabolic problems, see [3].

No propagation of the support. The theory for total variation flow predicts no propagation of support of the initial datum, if the support is regular enough. We recall that the total variation flow corresponds to the case of fluid viscosity equal to zero, therefore it is reasonable to expect that the propagation of the support depends on the value of the fluid viscosity, see Figures 5, 10, 15, 20, and 25. Our simulations indeed reflect these mathematical properties. In Cases I, II and III, the support of the initial datum is very regular (either a ball or two disjoint balls). The results obtained in these cases for the smaller viscosity value, namely $\mu = 0.0025$, show almost no propagation of support of the initial datum, as shown in Figures 2 and 4 for Case I; Figures 7, and 9 for Case II; Figures 12, and 14 for Case III. In Cases IV and V we see a change in topology of the support. More precisely, the support of the initial datum in Case IV is made of two disjoint disks whose boundaries are quite close to each other. The time evolution of the normalized solution $u(t,x)/\|u\|_{L^2(\Omega)}(t)$ shows that the two disks progressively merge, see Figures 17 and 19 and, finally, the support of the normalized solution at the extinction time has the shape of an hour-glass. In Case V, the support of the initial datum is a square while, at the extinction time, the support of the normalized solution is a disk, see Figures 22 and 25.

4.3 Conclusions on the numerical experiences

In this section we have presented some numerical results related to Bingham flow in a cylinder. In the limiting case of fluid viscosity equal to zero, the problem reduces to a total variation flow problem, in which solutions go to zero in a finite (extinction) time and there is no propagation of the support of the initial datum (if the support is regular enough).

Our simulations, for the special case of $f \equiv 0$ and $C \equiv 0$, show that similar qualitative properties hold also in the case of non-zero viscosity. We have considered two different viscosity values, $\mu = 0.25$ [Pa s] and $\mu = 0.0025$ [Pa s], and five different initial conditions, see Section 4.1, and we have solved the corresponding Bingham flow problem using a backward Euler scheme in combination with an algorithm á la Uzawa.

Our results showed existence of a finite extinction time, as predicted by the theory. We also found that the extinction time increases as the fluid viscosity decreases, as expected. This is due to the fact that a less

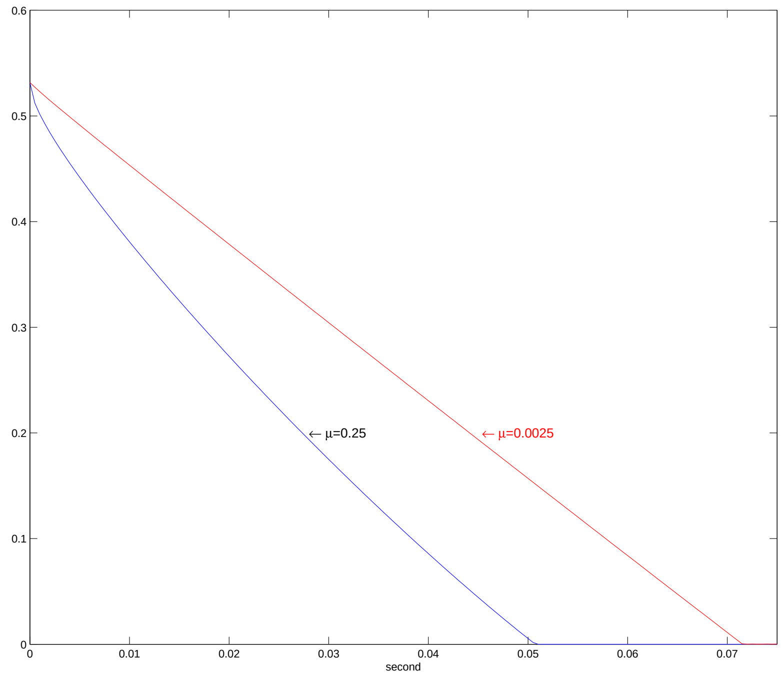

Figure 1. Case I - Time evolution of $\|u\|_{L^2(\Omega)}(t)$ for $\mu = 0.25$ and $\mu = 0.0025$ [Pa s].

viscous system has a less efficient dissipative mechanism and therefore it takes longer for the solution to decay to zero.

The theory for total variation flow also predicts no propagation of support of the initial datum, if the support is regular enough. In order to study this property, we visualized the time evolution of the normalized velocity $u(t,x)/\|u\|_{L^2(\Omega)}(t)$, for the different initial conditions and viscosity values. When the support of the initial datum is very regular (either a ball or two distant disjoint balls), the results corresponding to the smaller viscosity value, namely $\mu = 0.0025$, show almost no propagation of support of the initial datum, as predicted by the theory. When the support of the initial datum is not very regular (two close disjoint balls or a square), our results show a change in topology of the support.

Our simulations, for the special case of C large enough illustrate, numerically, the content of Theorem 4: if C is large enough the stabilization, as t goes to infinity, take place through a nontrivial solution of the stationary problem and the dynamics does not stop in any finite time.

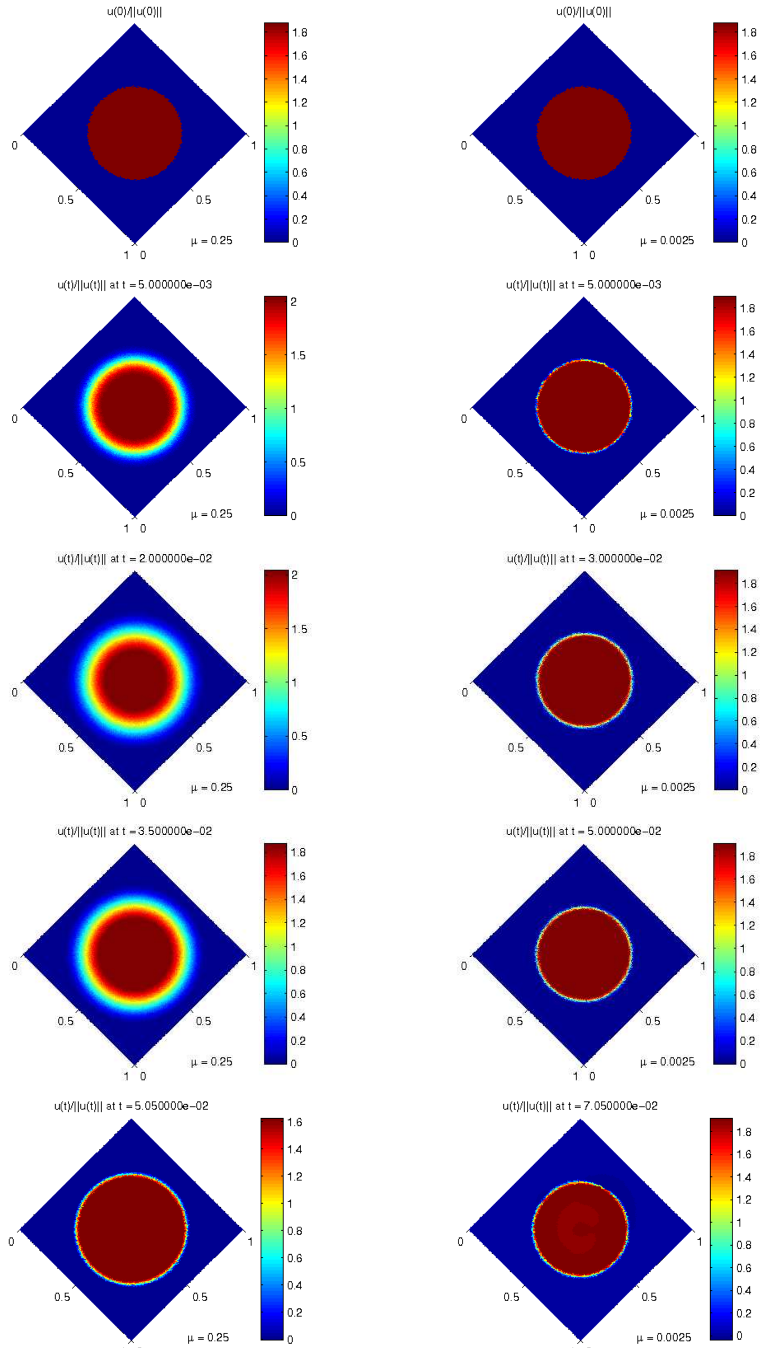

Figure 2. Case I - *On the left:* Snapshots of the normalized solution $u(t,x)/\|u\|_{L^2(\Omega)}(t)$ obtained with $\mu = 0.25$ at $t = 0,\ 0.005,\ 0.02,\ 0.035,\ 0.0505$ seconds; *On the right:* Snapshots of the normalized solution $u(t,x)/\|u\|_{L^2(\Omega)}(t)$ obtained with $\mu = 0.0025$ at $t = 0,\ 0.005,\ 0.03,\ 0.05,\ 0.0705$ seconds.

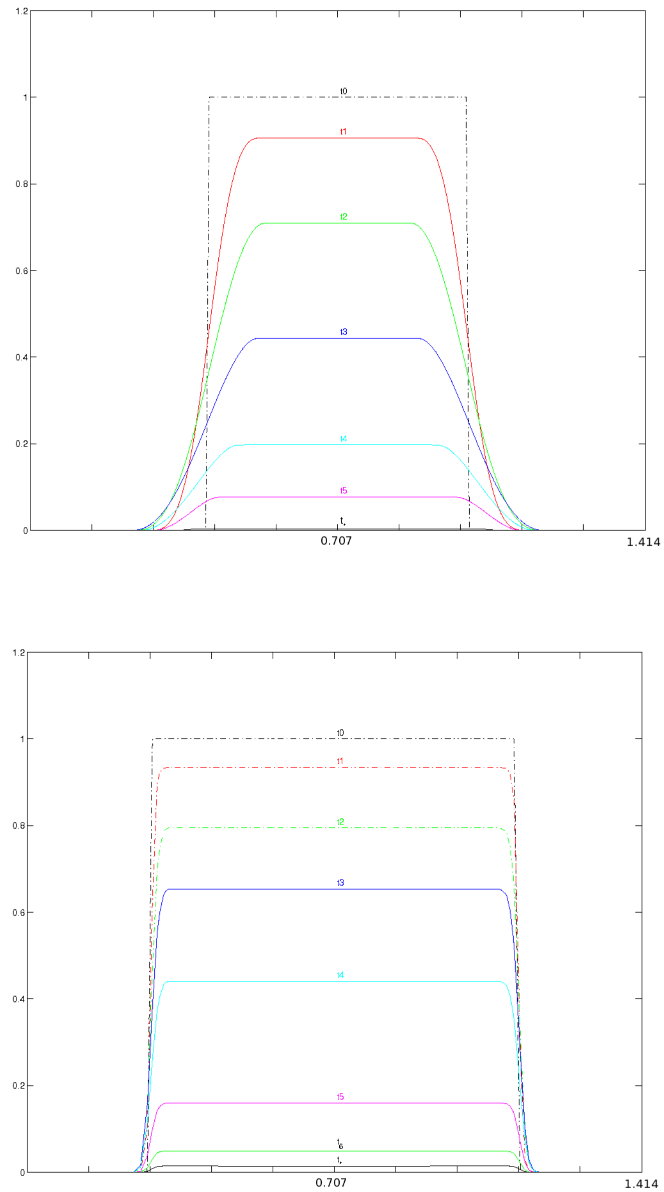

Figure 3. Case I - *On the top:* Snapshots of the solution $u(t,x)$ restricted to the domain diagonal obtained with $\mu = 0.25$ at $t_0 = 0$, $t_1 = 0.005$, $t_2 = 0.0135$, $t_3 = 0.025$, $t_4 = 0.0375$, $t_5 = 0.045$, $t^* = 0.0505$ seconds; *On the bottom:* Snapshots of the solution $u(t,x)$ restricted to the domain diagonal obtained with $\mu = 0.0025$ at $t_0 = 0$, $t_1 = 0.005$, $t_2 = 0.015$, $t_3 = 0.025$, $t_4 = 0.04$, $t_5 = 0.06$, $t_6 = 0.068$, $t^* = 0.0705$ seconds.

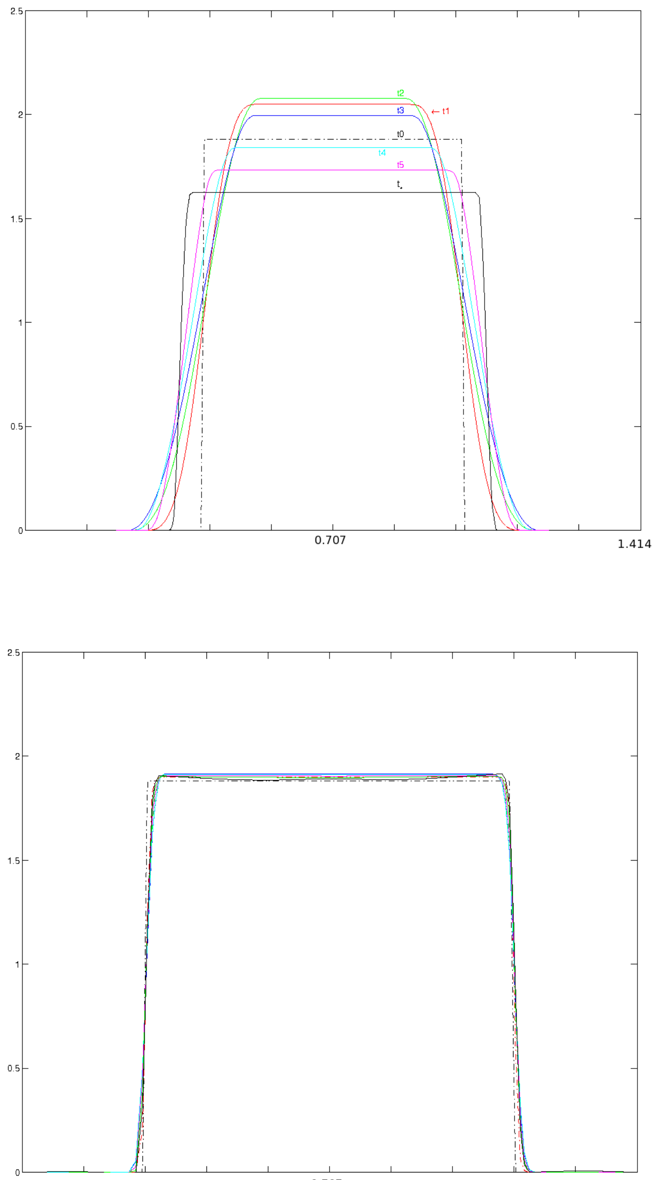

Figure 4. Case I - *On the top:* Snapshots of the normalized solution $u(t,x)/\|u\|_{L^2(\Omega)}(t)$ restricted to the domain diagonal obtained with $\mu = 0.25$ at $t_0 = 0$, $t_1 = 0.005$, $t_2 = 0.0135$, $t_3 = 0.025$, $t_4 = 0.0375$, $t_5 = 0.045$, $t^* = 0.0505$ seconds; *On the bottom:* Snapshots of the normalized solution $u(t,x)/\|u\|_{L^2(\Omega)}(t)$ restricted to the domain diagonal obtained with $\mu = 0.0025$ at $t_0 = 0$, $t_1 = 0.005$, $t_2 = 0.015$, $t_3 = 0.025$, $t_4 = 0.04$, $t_5 = 0.06$, $t_6 = 0.068$, $t^* = 0.0705$ seconds.

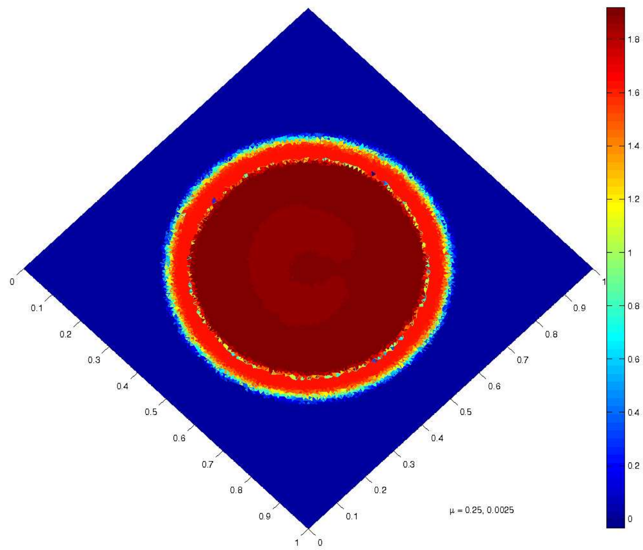

Figure 5. Case I - Comparison between the supports of the normalized solutions at extinction time obtained with $\mu = 0.25$ (outer circle) and with $\mu = 0.0025$ (inner circle).

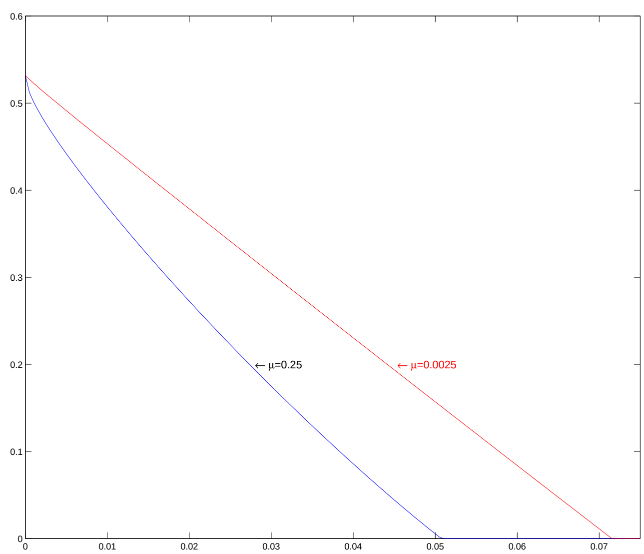

Figure 6. Case II - Time evolution of $\|u\|_{L^2(\Omega)}(t)$ for $\mu = 0.25$ and $\mu = 0.0025$ [Pa s].

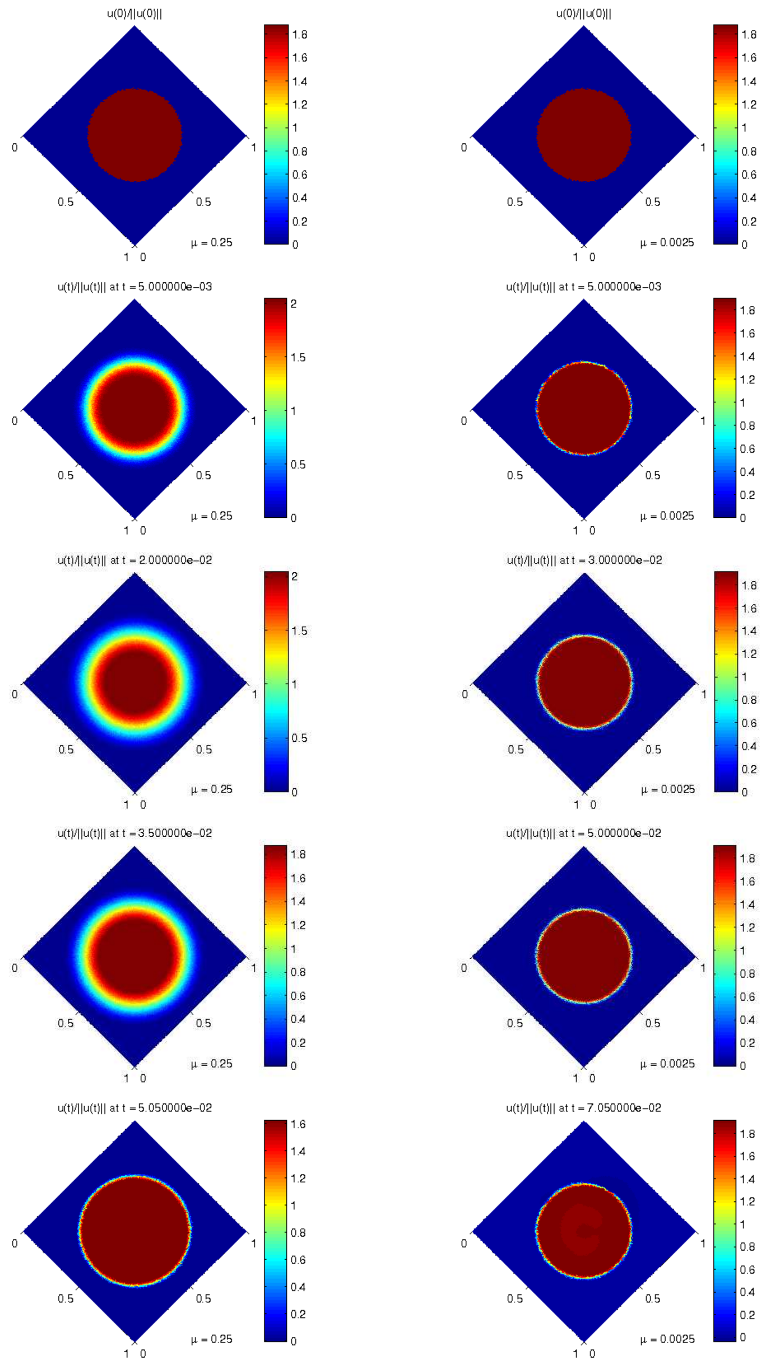

Figure 7. Case II - *On the left:* Snapshots of the normalized solution $u(t,x)/\|u\|_{L^2(\Omega)}(t)$ obtained with $\mu = 0.25$ at $t = 0$, 0.005, 0.03, 0.05, 0.071 seconds; *On the right:* Snapshots of the normalized solution $u(t,x)/\|u\|_{L^2(\Omega)}(t)$ obtained with $\mu = 0.0025$ at $t = 0$, 0.005, 0.004, 0.075, 0.1025 seconds.

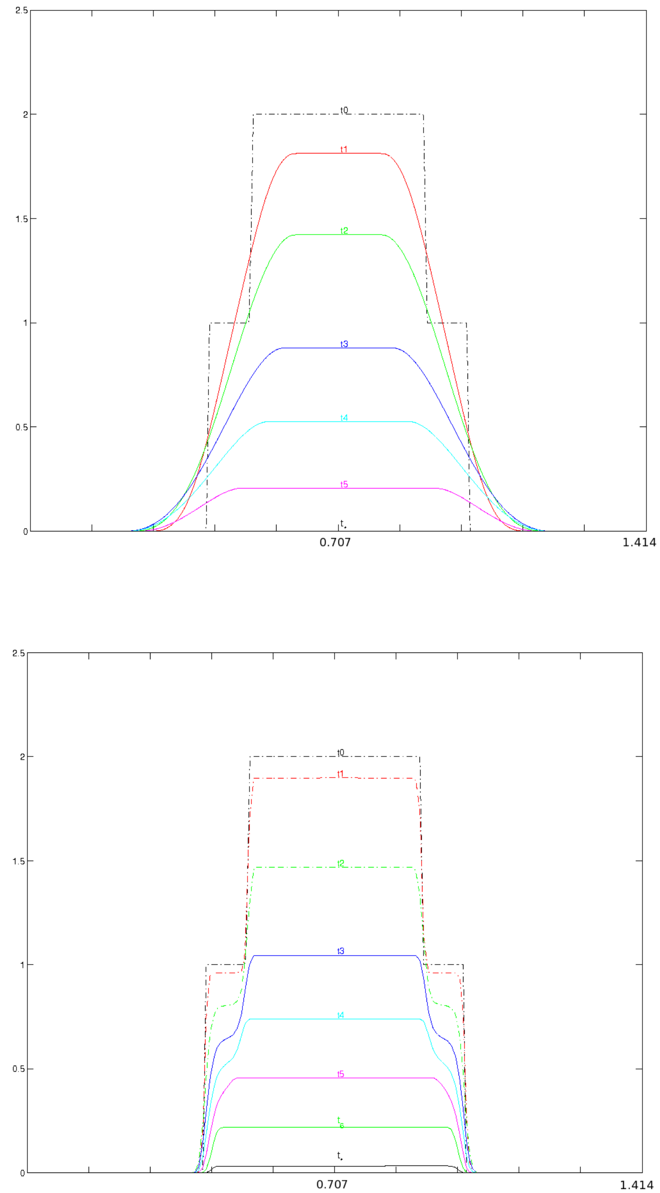

Figure 8. Case II - *On the top:* Snapshots of the solution $u(t,x)$ restricted to the domain diagonal obtained with $\mu = 0.25$ at $t_0 = 0$, $t_1 = 0.0055$, $t_2 = 0.015$, $t_3 = 0.003$, $t_4 = 0.0425$, $t_5 = 0.0575$, $t^* = 0.071$ seconds; *On the bottom:* Snapshots of the solution $u(t,x)$ restricted to the domain diagonal obtained with $\mu = 0.0025$ at $t_0 = 0$, $t_1 = 0.0045$, $t_2 = 0.0245$, $t_3 = 0.0445$, $t_4 = 0.0595$, $t_5 = 0.0745$, $t_6 = 0.095$, $t^* = 0.1025$ seconds.

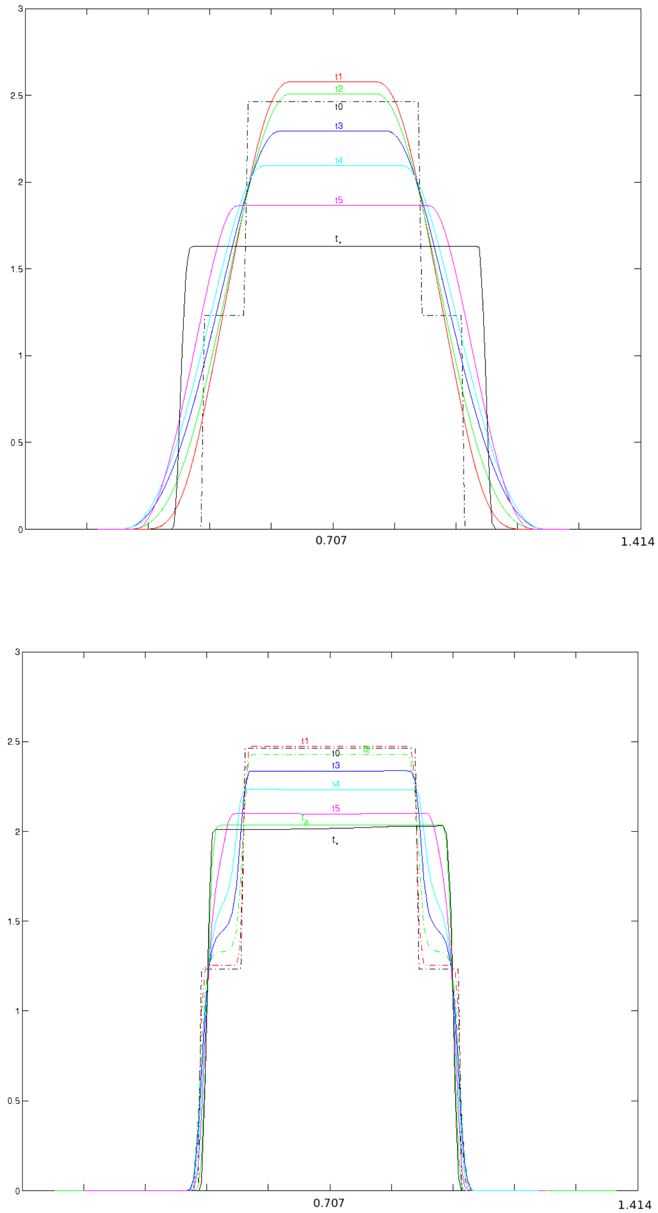

Figure 9. Case II - *On the top:* Snapshots of the normalized solution $u(t,x)/\|u\|_{L^2(\Omega)}(t)$ restricted to the domain diagonal obtained with $\mu = 0.25$ at $t_0 = 0$, $t_1 = 0.0055$, $t_2 = 0.015$, $t_3 = 0.003$, $t_4 = 0.0425$, $t_5 = 0.0575$, $t_* = 0.071$ seconds; *On the bottom:* Snapshots of the normalized solution $u(t,x)/\|u\|_{L^2(\Omega)}(t)$ restricted to the domain diagonal obtained with $\mu = 0.0025$ at $t_0 = 0$, $t_1 = 0.0045$, $t_2 = 0.0245$, $t_3 = 0.0445$, $t_4 = 0.0595$, $t_5 = 0.0745$, $t_6 = 0.095$, $t_* = 0.1025$ seconds.

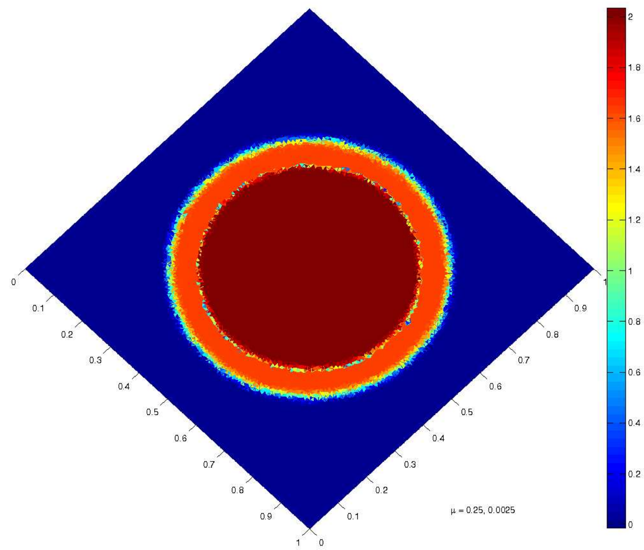

Figure 10. Case II - Comparison between the supports of the normalized solutions at extinction time obtained with $\mu = 0.25$ (outer circle) and with $\mu = 0.0025$ (inner circle).

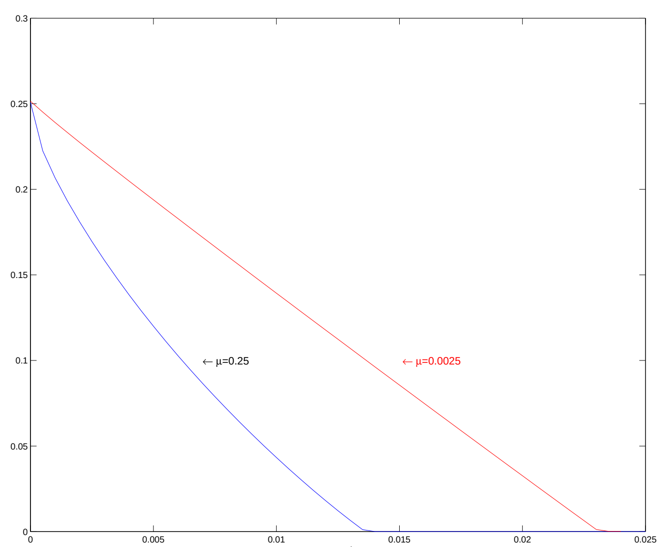

Figure 11. Case III - Time evolution of $\|u\|_{L^2(\Omega)}(t)$ for $\mu = 0.25$ and $\mu = 0.0025$ [Pa s].

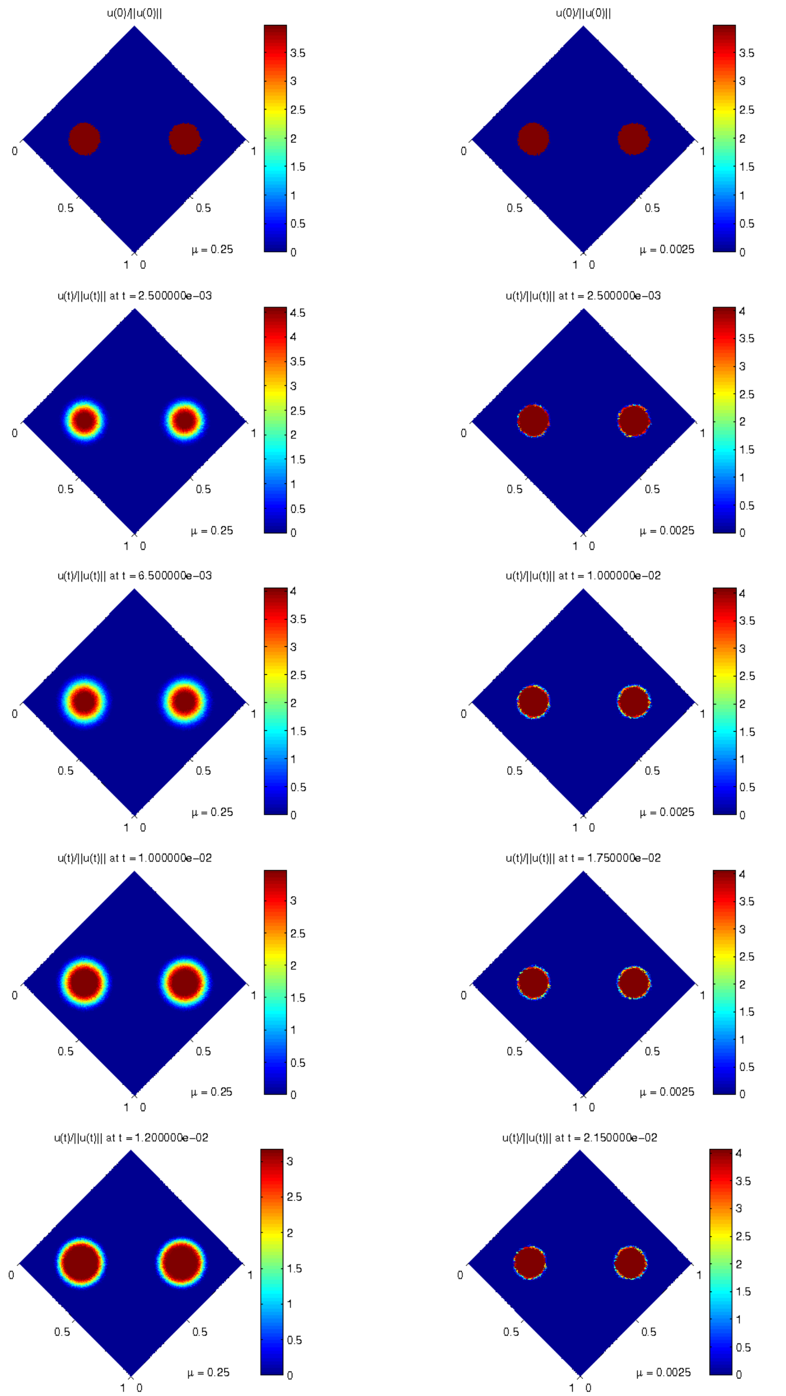

Figure 12. Case III - *On the left:* Snapshots of the normalized solution $u(t,x)/\|u\|_{L^2(\Omega)}(t)$ obtained with $\mu = 0.25$ at $t = 0$, 0.0025, 0.0065, 0.01, 0.012 seconds; *On the right:* Snapshots of the normalized solution $u(t,x)/\|u\|_{L^2(\Omega)}(t)$ obtained with $\mu = 0.0025$ at $t = 0$, 0.0025, 0.01, 0.0175, 0.0215 seconds.

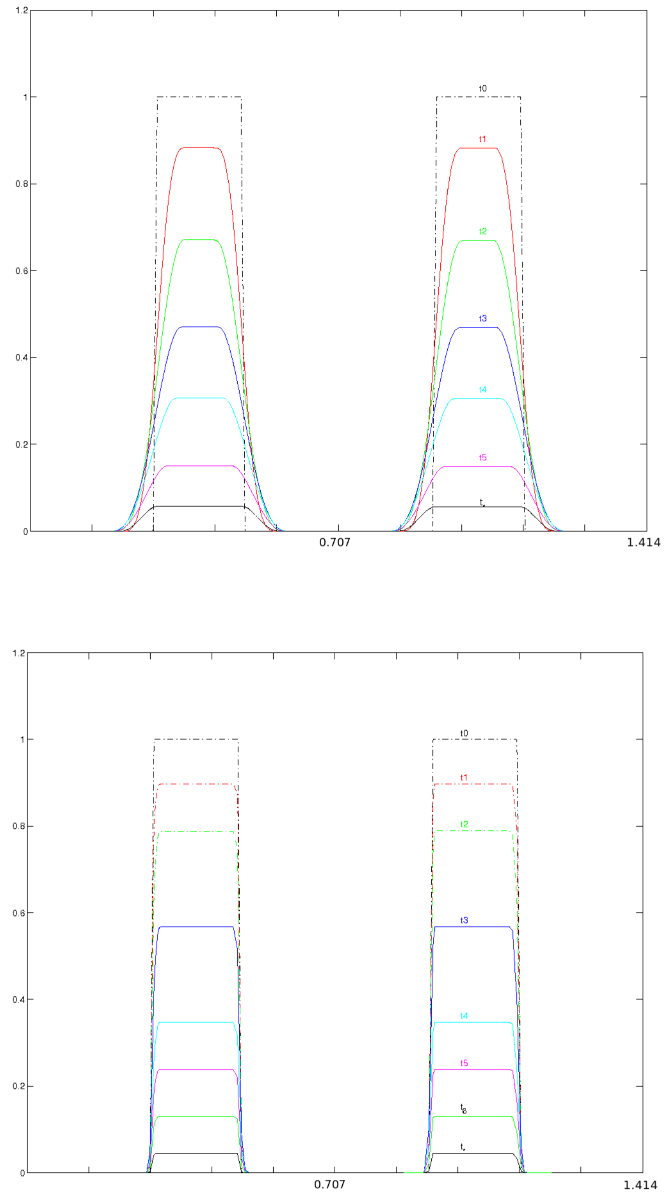

Figure 13. Case III - *On the top:* Snapshots of the solution $u(t,x)$ restricted to the domain diagonal obtained with $\mu = 0.25$ at $t_0 = 0$, $t_1 = 0.002$, $t_2 = 0.004$, $t_3 = 0.0065$, $t_4 = 0.009$, $t_5 = 0.0115$, $t_* = 0.012$ seconds; *On the bottom:* Snapshots of the solution $u(t,x)$ restricted to the domain diagonal obtained with $\mu = 0.0025$ at $t_0 = 0$, $t_1 = 0.0025$, $t_2 = 0.005$, $t_3 = 0.01$, $t_4 = 0.015$, $t_5 = 0.0175$, $t_6 = 0.02$, $t_* = 0.0215$ seconds.

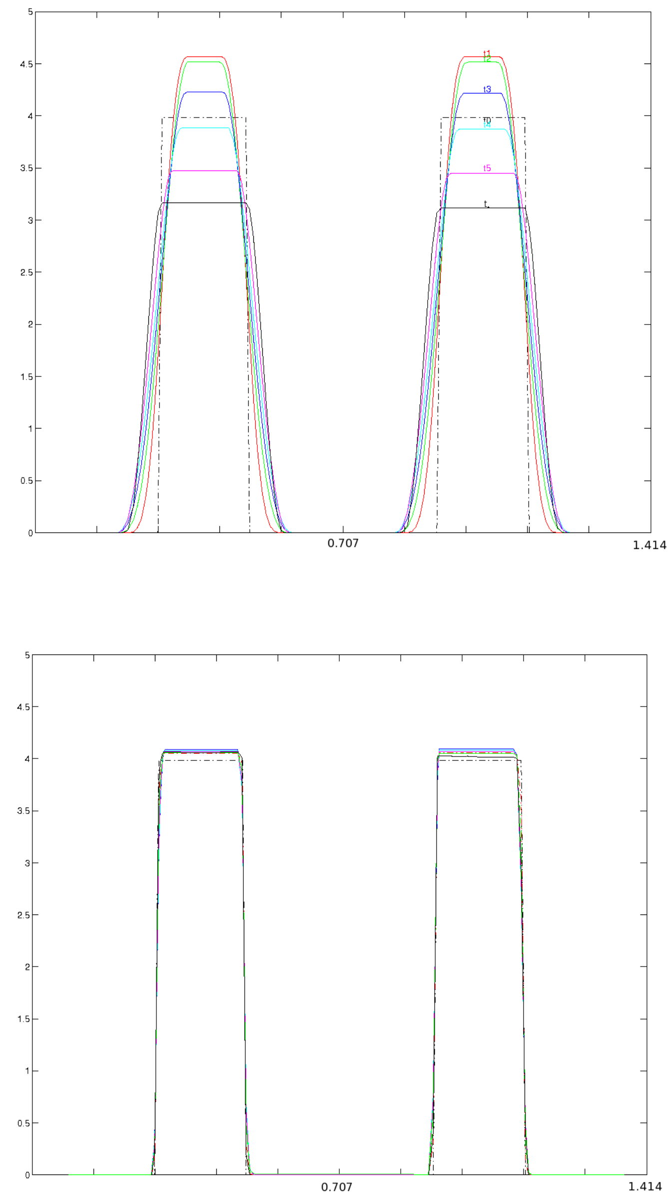

Figure 14. Case III - *On the top:* Snapshots of the normalized solution $u(t,x)/\|u\|_{L^2(\Omega)}(t)$ restricted to the domain diagonal obtained with $\mu = 0.25$ at $t_0 = 0$, $t_1 = 0.002$, $t_2 = 0.004$, $t_3 = 0.0065$, $t_4 = 0.009$, $t_5 = 0.0115$, $t_* = 0.012$ seconds; *On the bottom:* Snapshots of the normalized solution $u(t,x)/\|u\|_{L^2(\Omega)}(t)$ restricted to the domain diagonal obtained with $\mu = 0.0025$ at $t_0 = 0$, $t_1 = 0.0025$, $t_2 = 0.005$, $t_3 = 0.01$, $t_4 = 0.015$, $t_5 = 0.0175$, $t_6 = 0.02$, $t_* = 0.0215$ seconds.

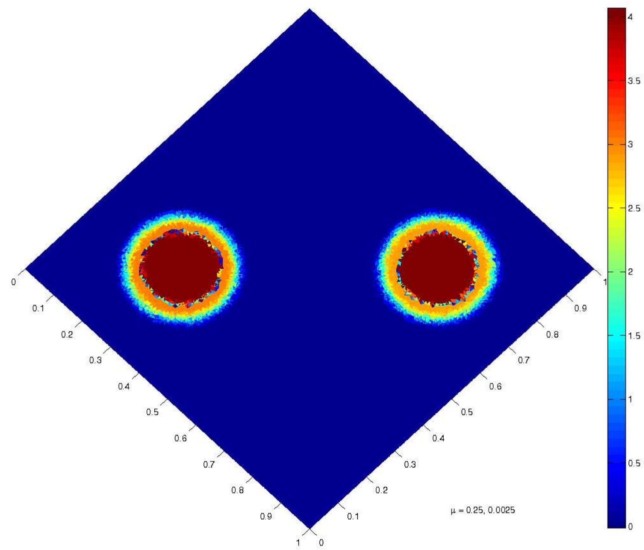

Figure 15. Case III - Comparison between the supports of the normalized solutions at extinction time obtained with $\mu = 0.25$ (outer circles) and with $\mu = 0.0025$ (inner circles).

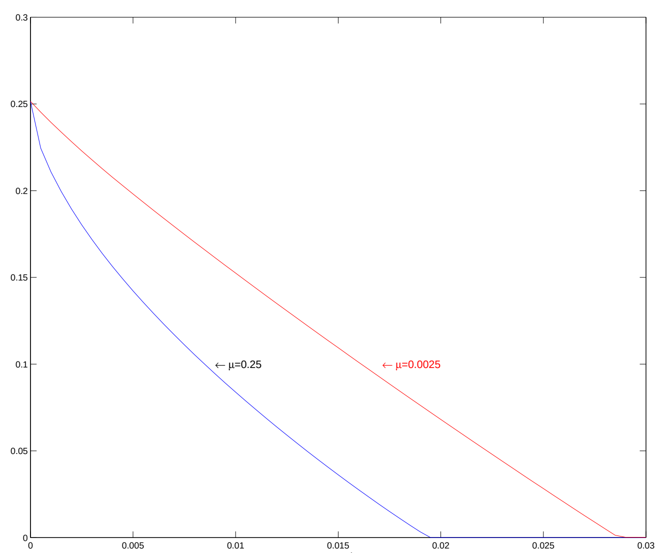

Figure 16. Case IV - Time evolution of $\|u\|_{L^2(\Omega)}(t)$ for $\mu = 0.25$ and $\mu = 0.0025$ [Pa s].

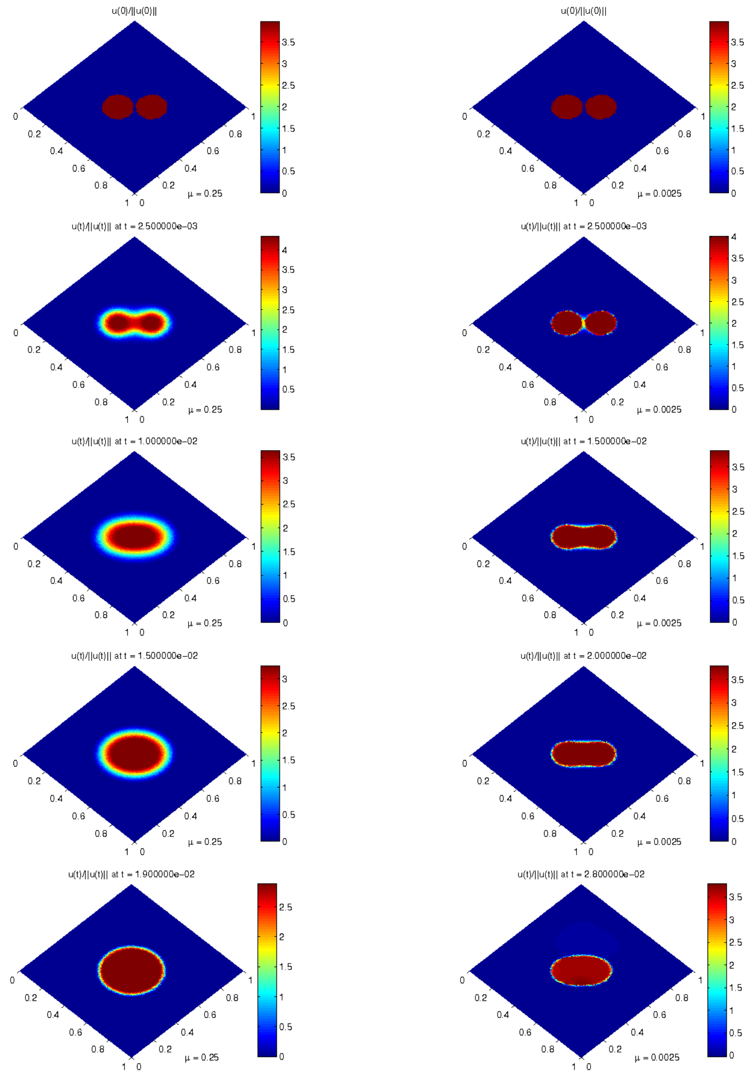

Figure 17. Case IV - *On the left:* Snapshots of the normalized solution $u(t,x)/\|u\|_{L^2(\Omega)}(t)$ obtained with $\mu = 0.25$ at $t = 0$, 0.0025, 0.01, 0.015, 0.019 seconds; *On the right:* Snapshots of the normalized solution $u(t,x)/\|u\|_{L^2(\Omega)}(t)$ obtained with $\mu = 0.0025$ at $t = 0$, 0.0025, 0.015, 0.02, 0.028 seconds.

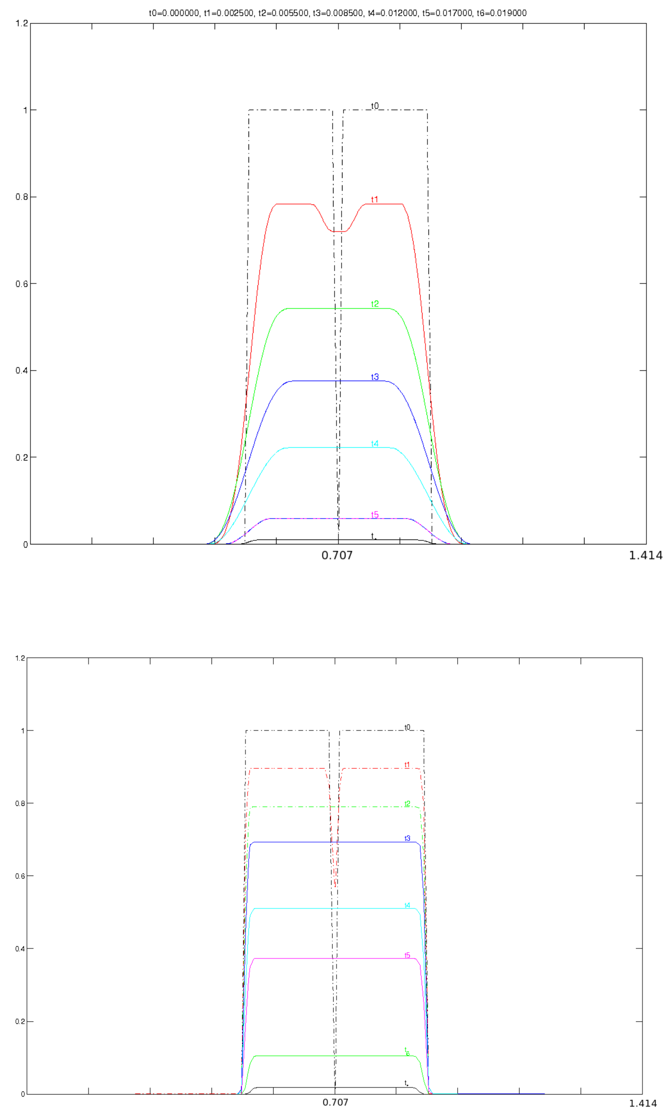

Figure 18. Case IV - *On the top:* Snapshots of the solution $u(t, x)$ restricted to the domain diagonal obtained with $\mu = 0.25$ at $t_0 = 0$, $t_1 = 0.0025$, $t_2 = 0.0055$, $t_3 = 0.0085$, $t_4 = 0.012$, $t_5 = 0.017$, $t_* = 0.019$ seconds; *On the bottom:* Snapshots of the solution $u(t, x)$ restricted to the domain diagonal obtained with $\mu = 0.0025$ at $t_0 = 0$, $t_1 = 0.0025$, $t_2 = 0.005$, $t_3 = 0.0075$, $t_4 = 0.0125$, $t_5 = 0.0165$, $t_6 = 0.025$, $t_* = 0.028$ seconds.

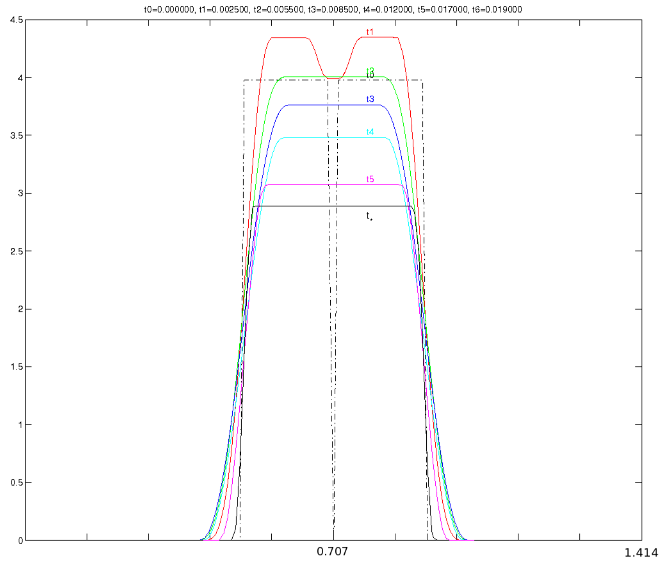

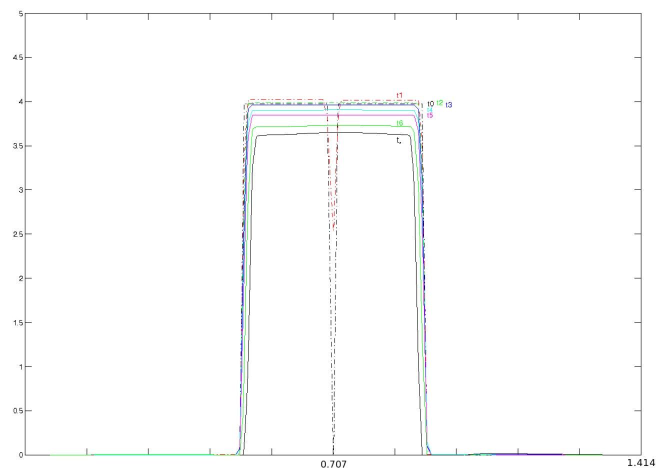

Figure 19. Case IV - *On the top:* Snapshots of the normalized solution $u(t,x)/\|u\|_{L^2(\Omega)}(t)$ restricted to the domain diagonal obtained with $\mu = 0.25$ at $t_0 = 0$, $t_1 = 0.0025$, $t_2 = 0.0055$, $t_3 = 0.0085$, $t_4 = 0.012$, $t_5 = 0.017$, $t_* = 0.019$ seconds; *On the bottom:* Snapshots of the normalized solution $u(t,x)/\|u\|_{L^2(\Omega)}(t)$ restricted to the domain diagonal obtained with $\mu = 0.0025$ at $t_0 = 0$, $t_1 = 0.0025$, $t_2 = 0.005$, $t_3 = 0.0075$, $t_4 = 0.0125$, $t_5 = 0.0165$, $t_6 = 0.025$, $t_* = 0.028$ seconds.

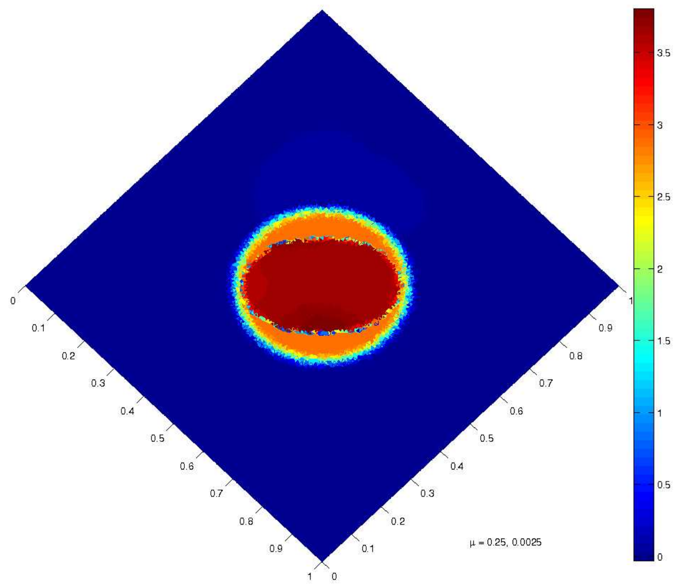

Figure 20. Case IV - Comparison between the supports of the normalized solutions at extinction time obtained with $\mu = 0.25$ (outer shape) and with $\mu = 0.0025$ (inner shape).

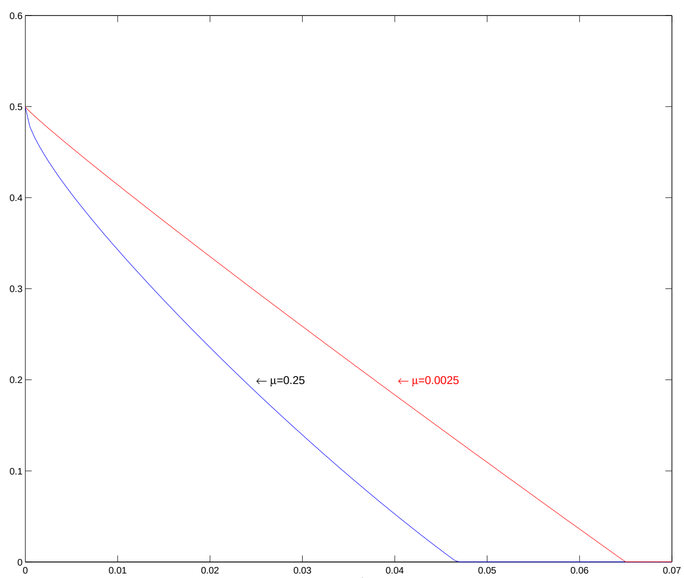

Figure 21. Case V - Time evolution of $\|u\|_{L^2(\Omega)}(t)$ for $\mu = 0.25$ and $\mu = 0.0025$ [Pa s].

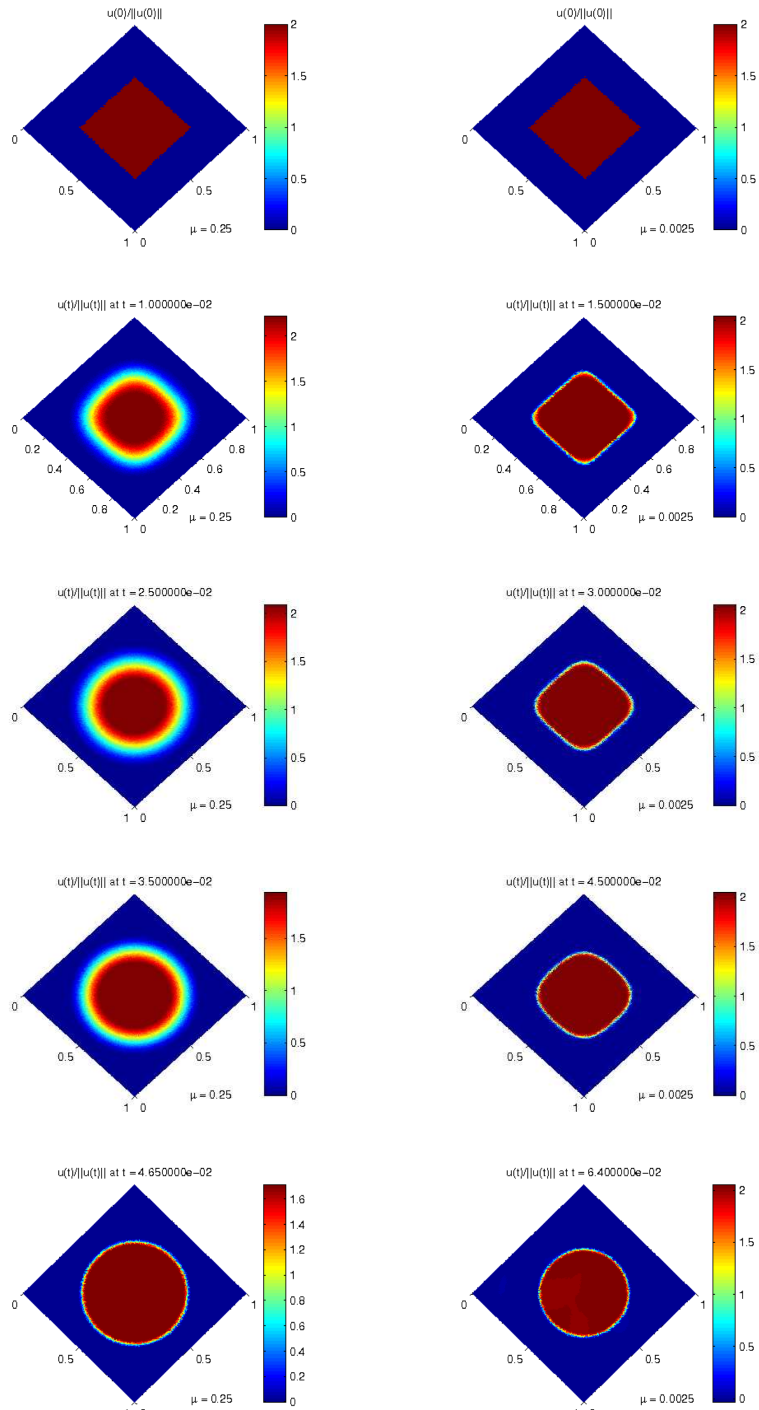

Figure 22. Case V - *On the left:* Snapshots of the normalized solution $u(t,x)/\|u\|_{L^2(\Omega)}(t)$ obtained with $\mu = 0.25$ at $t = 0$, 0.01, 0.025, 0.035, 0.045 seconds; *On the right:* Snapshots of the normalized solution $u(t,x)/\|u\|_{L^2(\Omega)}(t)$ obtained with $\mu = 0.0025$ at $t = 0$, 0.015, 0.03, 0.045, 0.064 seconds.

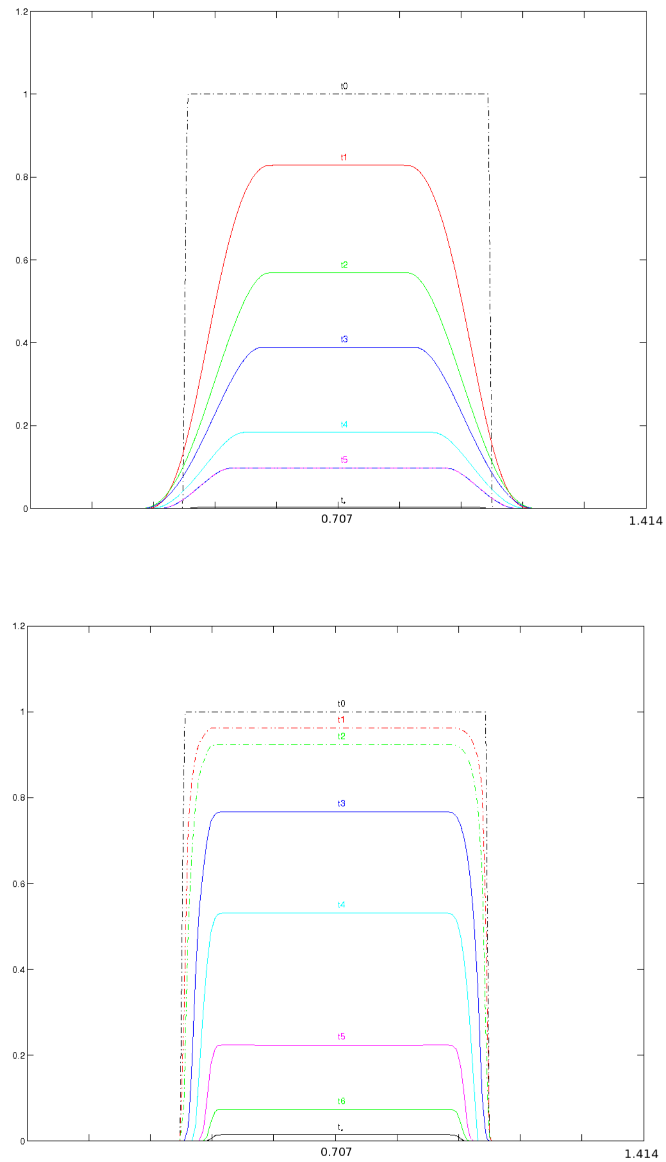

Figure 23. Case V - *On the top:* Snapshots of the solution $u(t, x)$ restricted to the domain diagonal obtained with $\mu = 0.25$ at $t_0 = 0$, $t_1 = 0.0075$, $t_2 = 0.0175$, $t_3 = 0.025$, $t_4 = 0.035$, $t_5 = 0.04$, $t_* = 0.0465$ seconds; *On the bottom:* Snapshots of the solution $u(t, x)$ restricted to the domain diagonal obtained with $\mu = 0.0025$ at $\mu = 0.0025$, $t_0 = 0$, $t_1 = 0.0025$, $t_2 = 0.005$, $t_3 = 0.015$, $t_4 = 0.03$, $t_5 = 0.05$, $t_6 = 0.06$, $t_* = 0.064$ seconds.

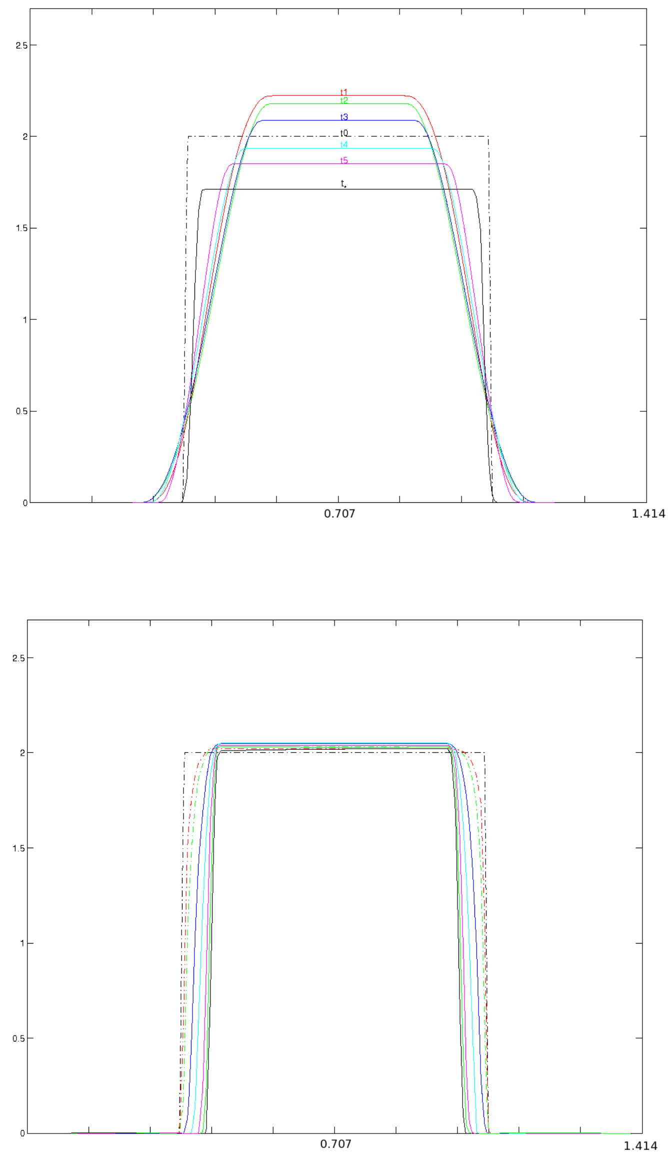

Figure 24. Case V - *On the top:* Snapshots of the normalized solution $u(t,x)/\|u\|_{L^2(\Omega)}(t)$ restricted to the domain diagonal obtained with $\mu = 0.25$ at $t_0 = 0$, $t_1 = 0.0075$, $t_2 = 0.0175$, $t_3 = 0.025$, $t_4 = 0.035$, $t_5 = 0.04$, $t_* = 0.0465$ seconds; *On the bottom:* Snapshots of the normalized solution $u(t,x)/\|u\|_{L^2(\Omega)}(t)$ restricted to the domain diagonal obtained with $\mu = 0.0025$ at $t_0 = 0$, $t_1 = 0.0025$, $t_2 = 0.005$, $t_3 = 0.015$, $t_4 = 0.03$, $t_5 = 0.05$, $t_6 = 0.06$, $t_* = 0.064$ seconds.

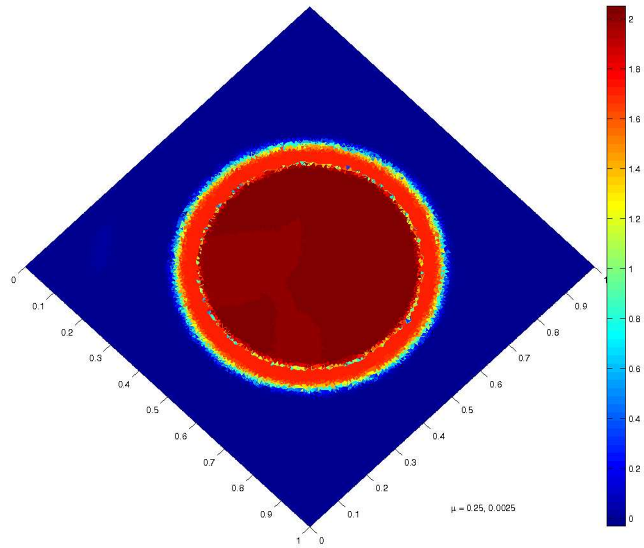

Figure 25. Case V - Comparison between the supports of the normalized solutions at extinction time obtained with $\mu = 0.25$ (outer circle) and with $\mu = 0.0025$ (inner circle).

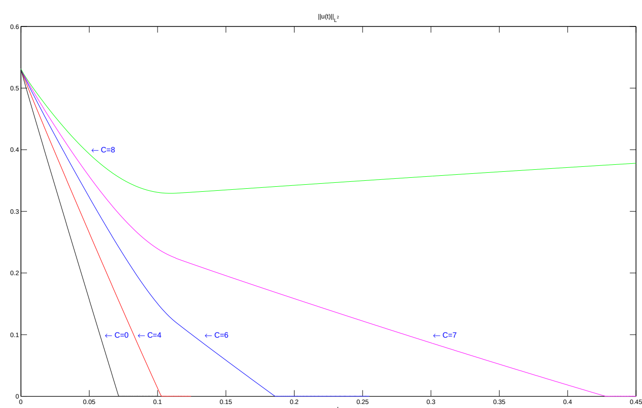

Figure 26. Case VI - Time evolution of $\|u\|_{L^2(\Omega)}(t)$ for different values of C.

Acknowledgement. The research of J. I. Díaz was partially supported by the project ref. MTM2008-06208 of the DGISPI (Spain), the Research Group MOMAT (Ref. 910480) supported by UCM. His research has received funding from the ITN "FIRST" of the Seventh Framework Programme of the European Community's, grant agreement number 238702. The research of R. Glowinski was partially supported by the NSF/DMS grant 0811138, NSF/NIH grant NIGMS/DMS 0443826 and by the NSF grant ATM 0417867. The research of G. Guidoboni was partially supported by the NSF/DMS grant 0811138 and the Texas Higher Education Board under grant ARP 003652-0051-2006. The research of T. Kim was partially supported by the NSF/DMS grant 0811138 and the Department of Mathematics of the University of Houston.

References

[1] ANDREU, F.; BALLESTER, C.; CASELLES, V. AND MAZÓN, J. M., (2001). Minimizing total variation flow, *Differential Integral Equations*, **14**, 321–360.

[2] ANDREU, F.; BALLESTER, C.; CASELLES, V. AND MAZÓN, J. M., (2001). The Dirichlet problem for the total variation flow, *J: Funct. Anal.*, **180**, 2, 347–403. DOI: 10.1006/jfan.2000.3698

[3] ANDREU, F.; CASELLES, V.; DÍAZ, J. I. AND MAZÓN, J. M., (2002). Some qualitative properties for the total variation flow, *J: Funct. Anal.*, **188**, 2, 516–547. DOI: 10.1006/jfan.2001.3829

[4] ANZELLOTTI, G., (1983). Paring between measures and bounded functions and compensated compactness, *Ann. Mat. Pura Appl. (4)*, **135**, 293–318.

[5] ANTONTSEV, S. N. AND DÍAZ, J. I., (1988). Applications of energy methods for localization of solutions of equations in Continuum Mechanics, *Dokl. Akad. Nauk SSSR. (Mathematical-Physics)*, **303**, 2, 320–325, (in russian). English trasslation *Soviet Phys. Dokl.*, **33**, 11, 813–816, (1989).

[6] ANTONTSEV, S. N. AND DÍAZ, J. I, (1989). Energy methods and localization of solutions for Continuum Mechanics Equations, *J. Appl. Mech. Tech. Phys.*, **174**, 2, 18–25, (in russian). DOI: 10.1007/BF00852162

[7] ANTONTSEV, S. N.; DÍAZ, J. I. AND SHMAREV, S. I., (2002). *Energy Methods for Free Boundary Problems: Applications to Nonlinear PDEs and Fluid Mechanics*, Progress in Nonlinear Differential Equations and Their Applications, **48**, Birkhäuser, Boston.

[8] BATCHELOR, G. K., (1967). *An introduction to fluid dynamics*, Cambridge University Press, Cambridge.

[9] BEGIS, D. AND GLOWINSKI, R., (1982). Application de la méthode des éléments finis à l'approximation d'un problème de domaine optimal, *R.A.I.R.O., Num. Anal.*, **16**, 351–373.

[10] BELLETTINI, G.; CASELLES, V. AND NOVAGA, M., (2002). The Total Variation Flow in R^N, *J. Differential Equations*, **184**, 475–525.

[11] BINGHAM, E. C., (1916). An Investigation of the Laws of Plastic Flow, *U.S. Bureau of Standards Bulletin*, **13**, 309–353.

[12] BREZIS, H., (1971). Monotonicity methods in Hilbert spaces and some applications to nonlinear partial differential equations. In: E. Zarantonello (Ed.), *Contributions to Nonlinear Functional Analysis*, Academic Press, New York, 101–156.

[13] BREZIS, H., (1973). *Operateurs maximaux monotones et semi-groupes de contractions dans les espaces de Hilbert* North-Holland, Amsterdam.

[14] CEA, J. AND GLOWINSKI, R., (1972). Méthodes numériques pour l'écoulement lamminare d'un fluide rigide visco-plastique incompressible, Int. J. Comput. Math., Section B, **3**, 225–255.

[15] DEAN, E. J.; GLOWINSKI, R. AND GUIDOBONI, G., (2007). On the numerical simulation of Bingham visco-plastic flow: Old and new results, *J. non-Newtonian Fluid Mech.*, **142**, 1–3, 36–62. DOI: 10.1016 /j.jnnfm.2006.09.002

[16] Díaz. J. I., (1992). Symmetrization of nonlinear elliptic and parabolic problems and applications: a particular overview. In C. Bandle et al. eds., *Progress in partial differential equations.elliptic and parabolic problems*, Pitman Research Notes in Mathematics Longman, Harlow, Essex, 1–16.

[17] Díaz, J. I. and de Thelin, F., (1994). On a nonlinear parabolic problems arising in some models related to turbulence flows, *SIAM J. Math. Anal.*, **25**, 4, 1085–1111. DOI: 10.1137/S0036141091217731

[18] Duvaut, G. and Lions, J. L., (1976). Inequalities in Mechanics an Physics, Springer, Berlin.

[19] Duvaut, G. Lions, J. L., (1972). Les Inéquations en Mécanique et Physique, Dunod, Paris.

[20] Friedman, A., (1964). *Partial differential equations of parabolic type*, Prentice-Hall, Englewood Cliffs, NJ.

[21] Glowinski, R., (1984). *Numerical Methods for Nonlinear Variational Problems*, Springer, New-York, NY.

[22] Glowinski, R., (2003). Finite element methods for incompressible viscous flow. In P. G. Ciarlet and J. L. Lions eds., *Handbook of Numerical Analysis*, **IX**, 3–1176, North-Holland, Amsterdam.

[23] Glowinski, R. and Le Tallec, P., (1989). Augmented Lagrangian interpretation of the nonoverlapping Schwarz alternating method. In: T. F. Chan, R. Glowinski, J. Périaux, O. B. Widlund (Eds.), *Proceedings of the Third International Symposium on Domain Decomposition Methods for Partial Differential Equations*, 224–231, Houston, TX, SIAM, Philadelphia, USA, 1990.

[24] Glowinski, R.; Lions, J. L. and Trémoliéres, R., (1981). *Numerical Analysis of Variational Inequalities*, North-Holland, Amsterdam.

[25] Hardt, M. and Zhou, X., (1998). *An evolution problem for linear growth functionals*, Interdisciplinary Applied Mathematics, **8**, Springer, New York.

[26] Kobayashi, R. and Giga, Y., (1999). Equations with singular diffusivity, *J. Statist. Phys.*, **95**, 1187–1220.

[27] Mossolov, P. P. and Miasnikov, V. P., (1965). Variational methods in the theory of fluidity of a viscus-plastic medium, *P. M. M.*, **29**, 468–492.

[28] Nakao, M., (1978). A difference inequality and its application to nonlinear evolution equations, *J. Math. Soc. Japan*, **30**, 4, 747–762. DOI: 10.2969/jmsj/03040747

[29] Rudin, L.; Osher, S. and Fatemi, E., (1992). Nonlinear total variation based noise removal algorithms, *Phys. D*, **60**, 259–268. DOI: 10.1016/0167-2789(92)90242-F

[30] Strauss, M. J., Variation of Korn's and Sobolev's inequalities. In, *Proceedings of Symposia in Pure Mathematics*, **23**, American Mathematics Society, Providence, RI., 1973, 207–214.

[31] Talenti, G., (1976). Best constant in Sobolev inequality. *Ann. Mat. Pura Appl. (4)*, **110**, 1, 353–372. DOI: 10.1007/BF02418013

[32] Waite, L. and Fine, J. M., (2007). *Applied Biofluid Mechanics*, McGraw-Hill Professional Publishing.

[33] Yosida, K., (1966). *Functional Analysis*, Springer-Verlag.

Jesús Ildefonso Díaz
Departamento de Matemática
Universidad Complutense de Madrid
Plaza de las Ciencias, 3
28040 Madrid, Spain
diaz.racefyn@insde.es
and
Real Academia de Ciencias Exactas, Físicas y Naturales
Valverde 22
28004 Madrid, Spain

Roland Glowinski
Department of Mathematics
University of Houston
PGH 651, Houston
Texas 77204-3476, USA
roland@math.uh.edu
and
Laboratoire Jacques-Louis Lions
Université P. et M. Curie
4 Place Jussieu, 75005, Paris, France

Giovanna Guidoboni
Department of Mathematics
University of Houston
PGH 651, Houston
Texas 77204-3476, USA
gio@math.uh.edu
and
Department of Mathematical Sciences
Indiana University and Purdue University at Indianapolis
402 N. Blackford St., LD270
Indianapolis, IN 46202-3267, USA

Taebeom Kim
Department of Mathematics
University of Houston
PGH 651, Houston
Texas 77204-3476, USA
taebeom@math.uh.edu